PALACIOS-FEST, M.R. 1996. Hohokam canal ostracode paleoenvironments from the McDowell-to-Shea sites; in: Henderson, T.K. and M. Hackbarth (eds.). Northland Research, Inc.

Chapter 21

HOHOKAM CANAL OSTRACODE PALEOENVIRONMENTS FROM THE McDOWELL-TO-SHEA SITES

Manuel R. Palacios-Fest

Prehistoric irrigation in Arizona influenced the basic characteristics of human settlement in the Phoenix Basin (Dart 1989). Population dynamics (such as population size, growth and density) were influenced by agricultural productivity. In turn, productivity was dependent upon the availability of water, its distribution among canal systems, and the placement of irrigation systems across the landscape (Dart 1989). To date, most models of Hohokam land use in the lower Salt River Valley have originated from examination of small portions of the prehistoric irrigation system (Cable and Doyel 1984, 1985; Cable and Mitchell 1988; Mitchell 1989). These studies concluded that land use and agricultural strategies changed through time. A close relationship between population growth and social complexity was stressed by these models.

Understanding the dynamics of Hohokam irrigation systems would allow archaeologists to examine the relationships between the evolution of social structure and agricultural activity. For example, Ackerly (1989c; Ackerly et al. 1987) suggested that periodic canal abandonment occurred due to Salt River channel instability. Nials et al. (1989) have also argued that frequent flooding caused significant canal damage which would have affected the Hohokam social structure.

The extent and constancy of the canal systems are critical issues for estimating the amount of irrigable land utilized by the Hohokam. Several attempts have been made to calculate the area of land irrigated by the Hohokam (Howard 1987; Midvale 1968; Nicholas 1981; Schroeder 1943; Turney 1929). These estimates, however, ignored the effect of seasonality in flow rates of the Salt River, and primarily assumed stability and long-term canal use. Other evidence has suggested that seasonal variation in water flow was a significant factor influencing the amount of water available for irrigation (Ackerly et al. 1987; Nials et al. 1989).

To examine the impact of seasonal variation on water availability, Henderson and Hackbarth (1993) proposed to study the physical, biological, and hand-crafted features associated with the canals found in the MTS project area. This study focuses on two goals: 1) to determine to what extent water availability is a result of seasonal variation; and 2) to estimate the efficiency of the irrigation systems and their growth over time. Ostracode paleoecology and shell chemistry are well suited for such an examination.

Previous examination of ostracode paleoecology from ancient Hohokam canals has provided important information toward understanding anthropogenic disturbance and climatic effects in the Phoenix Basin prior to European colonization (Palacios-Fest 1989, 1994a, 1994b). To date, little information exists to allow human impacts to be distinguished from climatic signatures in the geoarchaeologic record. Because the relative frequencies of ostracode species closely reflect the environmental conditions in which they lived, data from their paleoecology can be used to clarify impacts from human and natural actions. Ostracode paleoecology provides significant insights to address the following questions: What flow regimes are associated with the canals? Were the canals used seasonally? If so, what seasons? When were the canals abandoned?

The goal of this study is to make relative statements about how long a canal held water and how salinity and temperature changed through time based upon the ostracode assemblage composition and shell chemistry. The character of the canal water (e.g., active or sluggish flow) can also be discerned from variations in the presence and proportions of species adapted to either flowing stream conditions or standing water.

The MTS sites are unique because of the generally good preservation of ostracode fossils and geoarchaeologic features. Reconstruction of the canals' history, based on ostracode paleoecology and shell chemistry,

will allow us to understand water chemistry, intensity of land use, and anthropogenic effects on soils. Relative abundance and empirical paleosalinity indexes contribute proxy data to recognize canal operation patterns. Shell chemistry analysis provides geochemical information to estimate water temperature and salinity at the time of canal operation. Both paleoecologic and geochemical data allow us to detect cyclic agricultural events during the Hohokam occupation.

Recently, Palacios-Fest (1989, 1994a, 1994b) analyzed modern and ancient irrigation canals from northwestern Mexico (Magdalena, Sonora) and the southwestern United States as analogs for prehistoric canal systems. His monthly year-round modern canal studies allowed him to determine ostracode assemblage variations in response to both seasonal fluctuations and anthropogenic impact. Ostracode assemblages were observed to change throughout the year, mainly in response to the climate. However, some species (e.g., *Herpetocypris reptans*) are susceptible to human-induced water volume and flow changes that may cause waterlogging or salinization. Prehistoric canal ostracodes can provide critical information because they allow us to learn what environmental conditions were present when these organisms flourished. Based upon modern canal studies it is possible to characterize and differentiate between climatic and anthropogenic factors affecting ostracodes collected from ancient Hohokam canals.

Through experimental studies, Palacios-Fest (1994b) developed mathematical coefficients that can be used to reconstruct water paleotemperature and paleosalinity. These coefficients were calibrated internally within the experiments and with historic climatic records of the Phoenix Basin, from 1897 to the present (USDA records at the University of Arizona). They were then applied to the prehistoric Las Acequias canals' ostracode shell chemistry as a preliminary test of accuracy. These estimates were found to be reasonable and suggested seasonal canal operation within known salinity ranges (600–4,000 ppm of total dissolved solids [TDS]).

OSTRACODE CHARACTERISTICS

Ostracodes are microcrustaceans provided with a calcite carapace (Pokorný 1978). They inhabit a variety of aquatic (marine and nonmarine) ecosystems. Their life-cycles include seven to nine stages during which they shed their valves and form a new one after molting (Forester 1983). This process may be completed in less than an hour; however, complete calcification may require several hours (Palacios-Fest 1994b). As with most crustaceans, ostracode carapace replacement occurs between midnight and dawn, probably to avoid predation (Martha Palacios-Fest, personal communication 1994). During early stages, ostracodes form a high Mg-calcite carapace as calcification occurs rapidly; however, as they reach adulthood, slow calcification enables the formation of low Mg-calcite valves (Turpen and Angell 1971). Adult valves are most valuable for shell chemistry analysis because they most closely reflect environmental conditions (Chivas et al. 1983).

GEOLOGIC SETTING: AN OVERVIEW

The Scottsdale Canal System is a complex of Hohokam canals extending north of the Salt River to present day Scottsdale; the MTS canals are located near the head of the system, along State Route 87 within the Salt River Pima-Maricopa Indian Community (Figures 19.1 and 20.1). These canals were constructed by the Hohokam during the Classic (Features 1, 5, 20, and 23) and pre-Classic periods (Features 21, 22, and 24).

The study area lies along the terraces of the lower Salt River within the Basin and Range physiographic province. Péwé (1978) recognized four terraces of the Salt River in the Phoenix Basin (Lehi, Blue Point, Mesa, Sawick). Two of them, the Lehi (Holocene) and the Mesa (Pleistocene) terraces, are present in the project area.

The Lehi Terrace is poorly preserved within the project area because of its susceptibility to flooding and erosion. Three of the canals discussed in this study occur on the Lehi Terrace (Features 21, 22, 24); a fourth canal (historic Pima Lateral) on the terrace was not sampled for ostracodes because of flood deposits in the feature. Canals on the Lehi Terrace were subject to postabandonment alterations by flooding, but were prone to preservation by overbank flood deposits.

The Mesa Terrace canals were dug into cohesive clayey and $CaCO_3$-cemented soils (Huckleberry 1993). Today, these canals are visible on the terrace's surface and are more vulnerable to human and natural disturbance than the Lehi Terrace canals. Five canals occur on the Mesa Terrace (Features 1, 5, 6, 20, 23). All but Feature 6 will be examined in this chapter.

Canal sediments exhibit considerable variability. The canal cross sections included a variety of clays, silty clays, sandy clay loams, blocky clays, laminated clays or silts, sands, and gravelly deposits. Rodent burrows were common. Hackbarth (Chapter 19) and

Huckleberry (Chapter 20) discuss the stratigraphy and sediments of the canals in detail. Here, they are only mentioned to place the ostracodes in a lithologic perspective.

MATERIALS AND METHODS

Forty soil samples from the MTS canals were analyzed for ostracode content (Table 21.1). The samples were collected from seven canals located in two sites (AZ U:9:99, AZ U:9:100) along the north bank of the Salt River. Sampling intervals within canals were between 10 and 30 cm (Figures 19.16, 19.18, 19.21–19.23, 19.29). Because strongly disturbed intervals are unlikely to preserve ostracodes, these zones were not sampled. Ostracode samples were collected and numbered from the bottom to the top of each canal cross section as a means of avoiding possible contamination or mixing of sediment. Ostracode stratigraphic records are presented from bottom to top in Table 21.1, except for Feature 20 (Trench 47) where the sequence of sample numbers was reversed. Table 21.1 shows the stratigraphic sequence used in this study, as well as the position below datum.

Thirty-five of the 40 samples examined contained enough ostracodes for paleoecologic and geochemical analyses. Ostracode samples were selected to: 1) reconstruct individual canal history, 2) correlate equivalent strata between different canals, and 3) define periodicity (seasonality) of canal operation during the Hohokam occupation.

The sample preparation technique used is a modified version described by Forester (1991). Sediment residuals were analyzed under a low-power stereoscopic microscope. Routine paleontological study of all 35 fossiliferous samples was performed to determine fossil content and faunal assemblages. According to species abundance a paleosalinity index was used in this study to establish the canal operation history (see Palacios-Fest 1994a). This "qualitative" salinity index (SI) was developed based on the weighted average species proportions, as follows:

$$SI = 4(\%L.\ staplini) + 3(\%C.\ patzcuaro) + 2(\%C.\ vidua) + \%H.\ reptans - (\%I.\ bradyi + 2(\%C.\ ophthalmica) + 3(\%P.\ pustulosa) + 4(\%D.\ stevensoni)) \quad (1)$$

For geochemical analyses, 159 individual pristine valves of *Limnocythere staplini* were selected from all fossiliferous samples (4–5 specimens from each sample). Each valve was thoroughly washed in a 5 percent H_2O_2 solution at room temperature for about 30 minutes. Residuals were removed with a fine brush (000). Valves were carefully rinsed four times in <18 ΩOhm MQ water. Then, valves were individually weighed using a Cahn 29 electronic balance (±.002 μg) and dissolved in 3 ml of a 2 percent (.12 N) distilled HCl solution (prepared in the Isotope and Trace Element Laboratory of the Department of Geosciences, University of Arizona). Trace element analysis was performed in a Turner TS SOLA inductively coupled plasma argon mass spectrometer (ICP-MS). Mg^{2+} and Sr^{2+} concentrations were directly measured from each valve. Detection limits for these ions were .1 ppb; two sigma above background. All analyses were run against multi-element standards prepared from Spex™ stock solutions. Calcium content was determined stoichiometrically as a result of the instrument sensitivity to major elements like calcium. Trace element data were converted into molar ratios of Mg/Ca and Sr/Ca. These ratios were in turn used to generate paleoenvironmental estimates using Palacios-Fest's (1994b) experimentally derived equations (2) and (3):

$$T(°C) = \frac{m\left(\frac{Mg}{Ca}\right)_{valve} - \alpha_0}{\alpha_2} \quad (2)$$

$$S^0/_{00} = \frac{m\left(\frac{Sr}{Ca}\right)_{valve} - \beta_0}{\beta_1} \quad (3)$$

where α_0 = -.00083 and α_2 = .00074 for temperature, and $\beta_0 = 7 \times 10^{-5}$ and $\beta_1 = 2 \times 10^{-7}$ for salinity as ppm TDS.

THE CANAL OSTRACODES

Paleoecologic Record

Table 21.2 summarizes the species present and environmental conditions controlling ostracode assemblages occurring at the MTS sites. Eight recognized and one unknown species were observed in the canal sediments. The dominant species, *Limnocythere staplini* alternates with *Candona patzcuaro* or more rarely with

Table 21.1. Ostracode Samples Examined from the MTS Canals. (Page 1 of 2)

ASM Site	Feature	Trench	Terrace	Sample No.	Stratigraphic Position from Base (cm)	Stratigraphic Position below Datum (cm)	Other Plant Debris	Fossil Mollusks	Oogonia	Sediment Type	Sediment Color
AZ U:9:100	1	5	Mesa	NR-1-1-28	15	150	X	X	8	Gravelly sandy silt	Orange brown
				NR-1-3-37	35	120	X	X	1	Gravelly sandy silt	Orange brown
				NR-1-6-48	65	90	X	X	1	Gravelly sandy silt	Orange brown
				NR-1-7-53	75	70	X	X	0	Gravelly sandy silt	Orange brown
				NR-1-9-61	95	60	X	X	2	Sandy silty clay	Reddish brown
				NR-1-12-73	125	30	X	X	1	Sandy silty clay	Reddish dark brown
				NR-1-15-88	155	10	X	X	8	Sandy silty clay	Reddish dark brown
AZ U:9:100	5	10	Mesa	NR-5-C-3	35	30		X	0	Gravelly sand	Whitish red brown
				NR-5-1-8	3	70		X	0	Gravelly sandy silt	Reddish brown
				NR-5-3-15	15	50		X	0	Gravelly sandy clay	Reddish brown
				NR-5-5-23	35	30			0	Sandy silty clay	Whitish red brown
AZ U:9:99	20	47	Mesa	NR-20-1-8	55	5+	X	X	0	Sandy silty clay	Reddish dark brown
				NR-20-2-11	50	0	X	X	1	Sandy silty clay	Reddish dark brown
				NR-20-3-13	30	20	X	X	0	Sandy silty clay	Reddish dark brown
				NR-20-4-41	20	30	X	X	0	Sandy silty clay	Reddish dark brown
				NR-20-5-42	10	40	X	X	16	Sandy silty clay	Reddish dark brown
				NR-20-6-48	0	50	X	X	0	Sandy silty clay	Reddish dark brown
AZ U:9:99	21	91	Lehi	NR-21-1-428	7	125	X		0	Sandy silty clay	Dark brown
				NR-21-2-432	22	110	X		0	Sandy silty clay	Reddish dark brown
				NR-21-3-434	42	100	X		0	Sandy silty clay	Dark brown
				NR-21-4-439	72	75	X	X	0	Sandy silty clay	Reddish dark brown
AZ U:9:99	22	93	Lehi	NR-22-1-467	10	150	X		0	Sandy silty clay	Dark brown
				NR-22-2-471	20	135	X	X	0	Sandy silty clay	Reddish brown
				NR-22-3-474	30	125		X	0	Gravelly sandy silt	Whitish red brown
				NR-22-4-478	40	103		X	0	Sandy silty clay	Reddish brown
				NR-22-5-483	70	90			0	Sandy silty clay	Reddish brown
				NR-22-6-485	75	80	X	X	0	Fine sand/silt/clay	Reddish dark brown
				NR-22-7-490	88	67	X	X	0	Fine sand/silt/clay	Dark reddish brown
AZ U:9:99	23	81	Mesa	NR-23-1-450	10	60		X	4	Gravelly sandy silt	Reddish dark brown
				NR-23-2-452	33	40		X	4	Gravelly sandy silt	Reddish brown
				NR-23-3-455	40	32		X	8	Gravelly sandy silt	Orange brown
				NR-23-4-456	48	24		X	0	Gravelly sandy silt	Yellowish brown
				NR-23-5-459	55	18	X	X	0	Gravelly sandy silt	Yellowish brown

Table 21.1. Ostracode Samples Examined from the MTS Canals. (Page 2 of 2)

ASM Site	Feature	Trench	Terrace	Sample No.	Stratigraphic Position from Base (cm)	Stratigraphic Position below Datum (cm)	Other Plant Debris	Fossil Mollusks	Oogonia	Sediment Type	Sediment Color
AZ U:9:99	24	93	Lehi	NR-24-1-504	5	147		X	0	Sandy silty clay	Reddish dark brown
				NR-24-2-507	10	143			0	Sandy silty clay	Reddish dark brown
				NR-24-3-510	18	135			0	Sandy silty clay	Reddish dark brown
				NR-24-4-515	30	123			0	Gravelly sandy silt	Reddish dark brown
				NR-24-5-518	40	107			0	Gravelly sandy silt	Reddish dark brown
				NR-24-6-523	55	97	X	X	0	Sandy silty clay	Reddish dark brown
				NR-24-7-526	68	85	X	X	1	Gravelly sandy silt	Reddish dark brown

Table 21.2. Generalized Environmental Conditions of Ostracode Species in this Study.

Species[1]	Habitat	Life-cycle	Permanence	Temperature	Salinity	Chemistry
Limnocythere staplini	Lake or pond	4–6 weeks	Perennial or ephemeral	Thermophillic	500–75,000 ppm	Ca-rich waters
Cypridopsis vidua	Lake, pond or spring	4–8 weeks	Perennial or ephemeral	Eurythermic	100–4,000 ppm	Eurytopic
Candona sp. cf. *C. patzcuaro*	Lake or pond	10–16 weeks	Perennial or ephemeral	Eurythermic	200–5,000 ppm	Eurytopic
Ilyocypris bradyi	Stream or pond	10–16 weeks	Perennial or ephemeral	Thermophillic	100–4,000 ppm	Eurytopic
Herpetocypris reptans	Stream or pond	8–10 weeks	Perennial or ephemeral	Eurythermic	100–4,000 ppm	Freshwater to Ca-rich
Cypria ophthalmica	Stream or pond	4–8 weeks	Perennial or ephemeral	Eurythermic	200–5,000 ppm	Freshwater to Ca-rich
Physocypria pustulosa	Lake or pond	6–8 weeks	Perennial or ephemeral	Thermophillic	100–600 ppm	Freshwater to Ca-rich
Darwinula stevensoni	Lake or pond	>20–26 weeks	Perennial	Eurythermic	50–2,000 ppm	Freshwater to Ca-rich

[1] Unknown species not included

Cypridopsis vidua. Other species (*Herpetocypris reptans, Ilyocypris bradyi, Cypria ophthalmica, Physocypria pustulosa, Darwinula stevensoni*) and an unknown species (designated as Sp. 1) occur occasionally. Based on the occurrence and relative abundance of these species (Table 21.3), four assemblages were recognized (Table 21.4), all of them probably characterizing the water pathway types I (dilute) and II (Ca-enriched waters dominated additionally by Na^+, Mg^{2+}, and $SO_4^=$) of Eugster and Hardie (1978).

Hem (1985) shows that the Salt and Gila rivers contained near-equivalent proportions of bicarbonate and calcium, with the latter slightly dominant (Type I to Type II). Paleoecologic ostracode assemblages reflect this water pathway. Canal waters evolved from Type I to Type II through time. With increasing ionic concentration *Candona patzcuaro* decreased, allowing *Limnocythere staplini* to replace it.

Table 21.3 presents the ostracodes relative abundance and the paleosalinity index values. All fossil samples were characterized by a small to moderate population (10–820 organisms/g of sediment) and low diversity (two to eight species). Table 21.4 presents the four assemblages recognized from the relative abundance profiles.

Figures 21.1 through 21.7 synthesize the paleoecologic and relative abundance diagrams for each species per canal. The paleosalinity index scale used in this report indicates only relative salinity gradients among the MTS project canals. (Absolute salinity values estimated in ppm of TDS will be discussed in the following shell chemistry section.) The total abundance chart in the figures indicates ostracode population regardless of species identification. The relative frequency of individual species is followed by the paleosalinity index derived from these charts. The paleosalinity index is influenced by the species variability throughout the canal history. Notice that the scale of the paleosalinity index changes from figure to figure. Bar charts used in these figures illustrate the proportional occurrence of species per sample. Note that in some bar charts only the six most common species are represented.

Figure 21.1 shows the ostracode occurrence pattern throughout Feature 1. A maximum of five species occurred in this canal (Table 21.3, Figure 21.1). Three assemblages of species were represented during the canal's history. The system was initially characterized by assemblage III (*C. patzcuaro*-dominated), but the composition rapidly changed to assemblage I (*L. staplini*-dominated). Before reaching desiccation, assemblage II (near-equivalent proportions of *L. staplini-C. patzcuaro-C. vidua*) developed in this canal. The final developmental stage was a return to assemblage III.

Figure 21.2 presents the species occurrence patterns in Feature 5. Five species were recognized in this canal. The total abundance chart indicates that ostracode populations increased dramatically toward the end of the canal record. Relative abundance charts show that *L. staplini* decreased dramatically while the frequencies of other species increased. The paleosalinity index reflects the *L. staplini* decrease because this was the dominant species. The bar chart shows the proportional occurrence of these species present in this canal through its history. Although this feature remained within assemblage I (*L. staplini*-dominated), it became more diverse at the end of the record.

Figure 21.3 plots the species occurrence patterns observed in Feature 20. This is the only feature where all nine species recognized in the project area were present. *L. staplini, C. vidua, I. bradyi*, and *P. pustulosa* occurred in all six intervals, *C. patzcuaro*, *D. stevensoni* and *H. reptans* occurred in at least four samples, and *C. ophthalmica* and Sp. 1 appeared occasionally. The total abundance chart shows that ostracodes declined after an abrupt population bloom shortly after the canal was put into use (i.e., sample NR-20-5-42 was only 10 cm from the base of the canal). The individual species frequency graphs indicate that *L. staplini* vastly dominated this canal, but co-occurred with *C. vidua*. The dominance of *L. staplini* strongly influenced the paleosalinity index. The bar chart presents the proportional occurrence of the most prevalent species found in this canal and allow recognition of assemblage I (*L. staplini*-dominated) during this canal's history.

Figure 21.4 shows the ostracode occurrence patterns found in Feature 21. This is the richest canal, both in population and diversity, as shown by the total abundance and relative abundance charts. Up to eight species were found within this canal; the paleosalinity index illustrates the influence of this diverse fauna. Three assemblages were recognized through the course of the canal's record. During initial canal operation assemblage III, dominated by *C. patzcuaro*, entered the system and remained abundant. However, assemblage I (*L. staplini*-dominated), and eventually assemblage II (near-equivalent proportions of *L. staplini-C. patzcuaro-C. vidua*), replaced the original colonies through time.

Table 21.3. Ostracode Relative Abundance and Salinity Index for the MTS Canals. (Page 1 of 2)

Ref No.	Sample No.	Strat. Posit. from Base (cm)	Organisms/gm	*Limnocythere staplini* %	*Candona patzcuaro* %	*Cypridopsis vidua* %	*Herpetocypris reptans* %	*Ilyocypris bradyi* %	*Cypria ophthalmica* %	*Physocypria pustulosa* %	*Darwinula stevensoni* %	Unknown Sp. 1 %	Salinity Index[1]
1	NR-1-1-28	15	45	8	77	12	0	1	0	0	2	0	284
2	NR-1-3-37	35	272	24	60	13	0	1	0	0	2	0	297
3	NR-1-6-48	65	98	61	33	6	0	0	0	0	0	0	355
4	NR-1-7-53	75	56	57	39	4	0	0	0	0	0	0	354
5	NR-1-9-61	95	114	35	40	15	0	5	0	0	5	0	274
6	NR-1-12-73	125	80	50	47	3	0	0	0	0	0	0	347
7	NR-1-15-88	155	70	37	40	17	0	0	0	0	6	0	291
8	NR-5-C-3	35	0	0	0	0	0	0	0	0	0	0	0
9	NR-5-1-8	3	15	64	21	15	0	0	0	0	0	0	350
10	NR-5-3-15	15	42	48	33	19	0	0	0	0	0	0	329
11	NR-5-5-23	35	431	39	25	19	13	0	0	0	4	0	273
12	NR-20-1-8	55	143	90	1	4	0	3	0	1	0	1	369
13	NR-20-2-11	50	167	79	1	6	0	4	0	8	2	0	291
14	NR-20-3-13	30	225	67	3	10	1	9	0	4	6	0	261
15	NR-20-4-41	20	379	72	1	9	0	2	1	11	3	1	248
16	NR-20-5-42	10	436	82	0	10	1	1	1	1	3	1	350
17	NR-20-6-48	0	140	76	0	20	1	2	0	1	0	0	341
18	NR-21-1-428	7	310	27	50	5	14	3	0	0	2	0	272
19	NR-21-2-432	22	260	23	47	7	21	1	0	0	1	0	268
20	NR-21-3-434	42	820	49	22	9	14	2	0	2	2	0	276
21	NR-21-4-439	72	413	37	38	0	23	0	2	0	0	0	279
22	NR-22-1-467	10	168	86	2	10	2	0	0	0	0	0	371
23	NR-22-2-471	20	19	21	11	46	0	11	0	0	0	11	200
24	NR-22-3-474	30	64	14	66	11	6	3	0	0	0	0	278
25	NR-22-4-478	40	100	39	35	6	16	4	0	0	0	0	286
26	NR-22-5-483	70	613	64	22	2	11	1	0	0	0	0	336
27	NR-22-6-485	75	132	39	18	7	18	15	0	0	3	0	221
28	NR-22-7-490	88	113	6	71	0	23	0	0	0	0	0	259
29	NR-23-1-450	10	60	35	34	31	0	0	0	0	0	0	304
30	NR-23-2-452	33	182	77	0	13	2	3	5	0	0	0	318
31	NR-23-3-455	40	48	63	0	19	0	13	6	0	0	0	256
32	NR-23-4-456	48	64	94	0	3	0	0	3	0	0	0	372
33	NR-23-5-459	55	120	91	0	0	0	0	9	0	0	0	336
34	NR-24-1-504	5	0	0	0	0	0	0	0	0	0	0	0

Table 21.3. Ostracode Relative Abundance and Salinity Index for the MTS Canals. (Page 2 of 2)

Ref No.	Sample No.	Strat. Posit. from Base (cm)	Organisms/gm	*Limnocythere staplini* %	*Candona patzcuaro* %	*Cypridopsis vidua* %	*Herpetocypris reptans* %	*Ilyocypris bradyi* %	*Cypria ophthalmica* %	*Physocypria pustulosa* %	*Darwinula stevensoni* %	Unknown Sp. 1 %	Salinity Index[1]
35	NR-24-2-507	10	0	0	0	0	0	0	0	0	0	0	0
36	NR-24-3-510	18	10	63	13	12	0	12	0	0	0	0	300
37	NR-24-4-515	30	22	69	15	8	0	8	0	0	0	0	331
38	NR-24-5-518	40	23	36	55	9	0	0	0	0	0	0	327
39	NR-24-6-523	55	0	0	0	0	0	0	0	0	0	0	0
40	NR-24-7-526	68	0	0	0	0	0	0	0	0	0	0	0

[1] The salinity index is a qualitative number only reflecting salinity variations.

Table 21.4. Ostracode Assemblages and Paleoenvironments. (Page 1 of 2)

Sample	*L. staplini*	*Ca. patzcuaro*	*Cy. vidua*	*H. reptans*	*I. bradyi*	*C. ophthalmica*	*P. pustulosa*	*D. stevensoni*	Unknown Sp. 1	Environment
					ASSEMBLAGE I					
NR-1-6-48	1	2	3							Saline, long water permanence
NR-1-7-53	1	2	3							Saline, long water permanence
NR-5-1-8	1	2	3							Saline, long water permanence
NR-5-3-15	1	2	3							Saline, long water permanence
NR-24-3-510	1	2	3							Saline, long water permanence
NR-24-4-515	1	2	3							Saline, long water permanence
NR-5-5-23	1	2	3	4				5		Moderately saline, long water permanence
NR-21-3-434	1	2	4	3	5		5	5		Moderately saline, long water permanence
NR-22-4-478	1	2	4	3	5					Moderately saline, long water permanence
NR-22-5-483	1	2	4	3	5					Moderately saline, long water permanence
NR-22-6-485	1	2	5	3	4			6		Moderately saline, long water permanence
NR-20-1-8	1	4	2		3		5		6	Hypersaline, salt crust dilution (?)
NR-20-2-11	1	5	3		4		2	6		Hypersaline, salt crust dilution (?)
NR-20-3-13	1	6	2		3	7	5	4		Moderately saline, long water permanence
NR-20-4-41	1	6	3		5	7	2	4	8	Moderately saline, long water permanence
NR-20-5-42	1		2	4	5	6	7	3	8	Saline,increasing evaporation
NR-20-6-48	1		2	4	3		5			Hypersaline, stagnant water, dessication (?)
NR-22-1-467	1	3	2	3						Hypersaline, ephemeral
NR-23-2-452	1		2	5	4	3				Very saline, increasing evaporation, ephemeral
NR-23-3-455	1		2		3	4				Very saline, increasing evaporation, ephemeral
NR-23-4-456	1		2			2				Hypersaline, ephemeral
NR-23-5-459	1					2				Hypersaline, ephemeral
					ASSEMBLAGE II					
NR-1-12-73	1	1	2							Slightly saline, long water permanence
NR-21-4-439	1	1		2		3				Slightly saline, long water permanence
NR-23-1-450	1	1	1							Slightly saline, long water permanence

Table 21.4. Ostracode Assemblages and Paleoenvironments. (Page 2 of 2)

Sample	*L. staplini*	*Ca. patzcuaro*	*Cy. vidua*	*H. reptans*	*I. bradyi*	*C. ophthalmica*	*P. pustulosa*	*D. stevensoni*	Unknown Sp. 1	Environment
					ASSEMBLAGE III					
NR-1-3-37	2	1	3		5			4		Stream diluted waters, long water permanence
NR-1-9-61	2	1	3		4			4		Stream diluted waters, long water permanence
NR-1-15-88	2	1	3					4		Stream diluted waters, long water permanence
NR-21-1-428	2	1	4	3	4			5		Stream diluted waters, long water permanence
NR-21-2-432	2	1	4	3	5			5		Stream diluted waters, long water permanence
NR-22-3-474	2	1	3	4	5					Stream diluted waters, long water permanence
NR-24-5-518	2	1	3							Stream diluted waters, long water permanence
NR-1-1-28	3	1	2		5			4		Diluted waters, long water permanence
NR-22-7-490	3	1		2						Diluted waters, long water permanence
					ASSEMBLAGE IV					
NR-22-2-471	2	3	1		3				3	Slightly saline, near headgate

Note: Numbers 1 to 8 express ranked occurrence within sample.

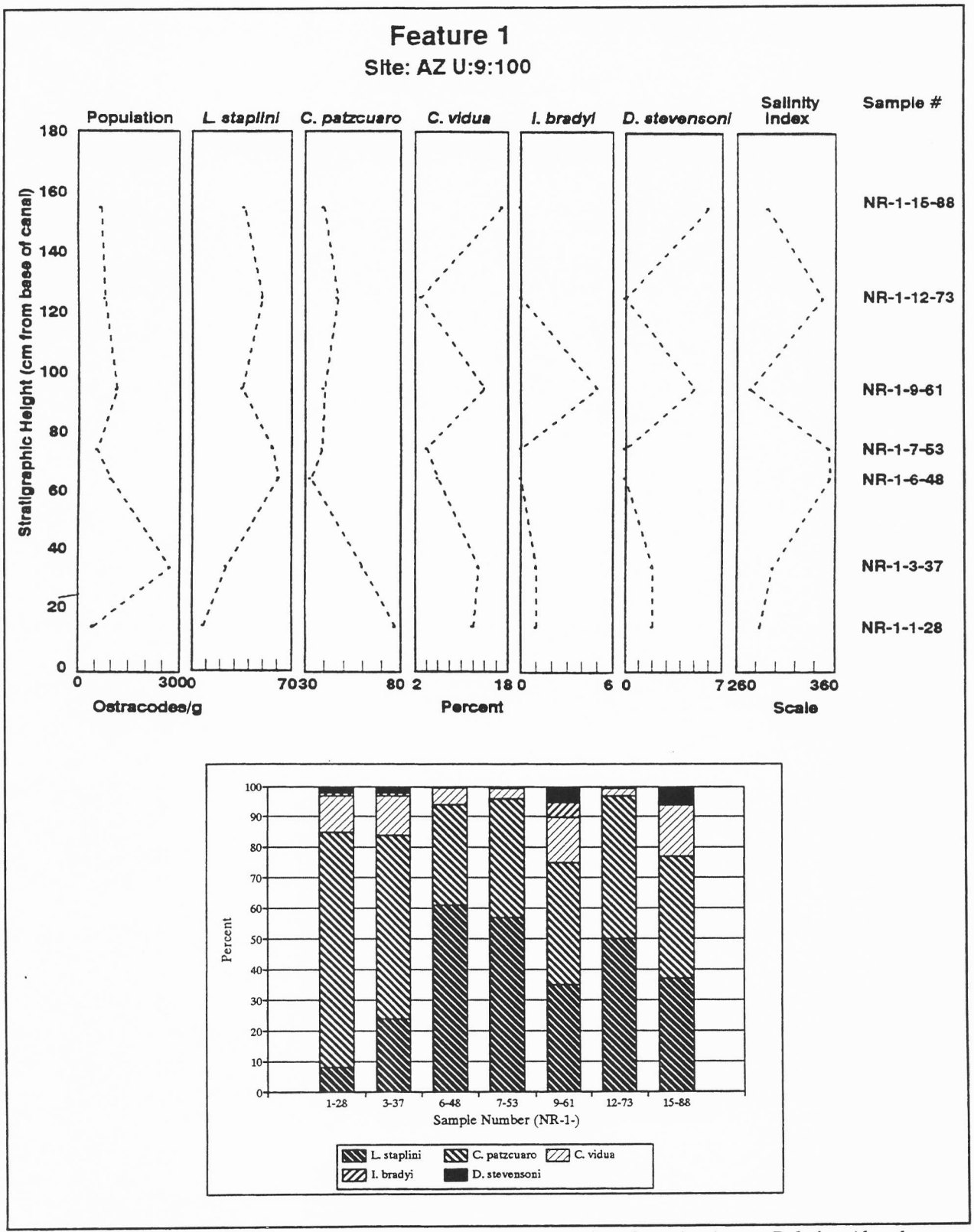

Figure 21.1 Ostracode Charts for Feature 1, AZ U:9:100, including Organism/gram, Relative Abundance by Species, Salinity Index, and Bar Chart of Relative Species Distribution.

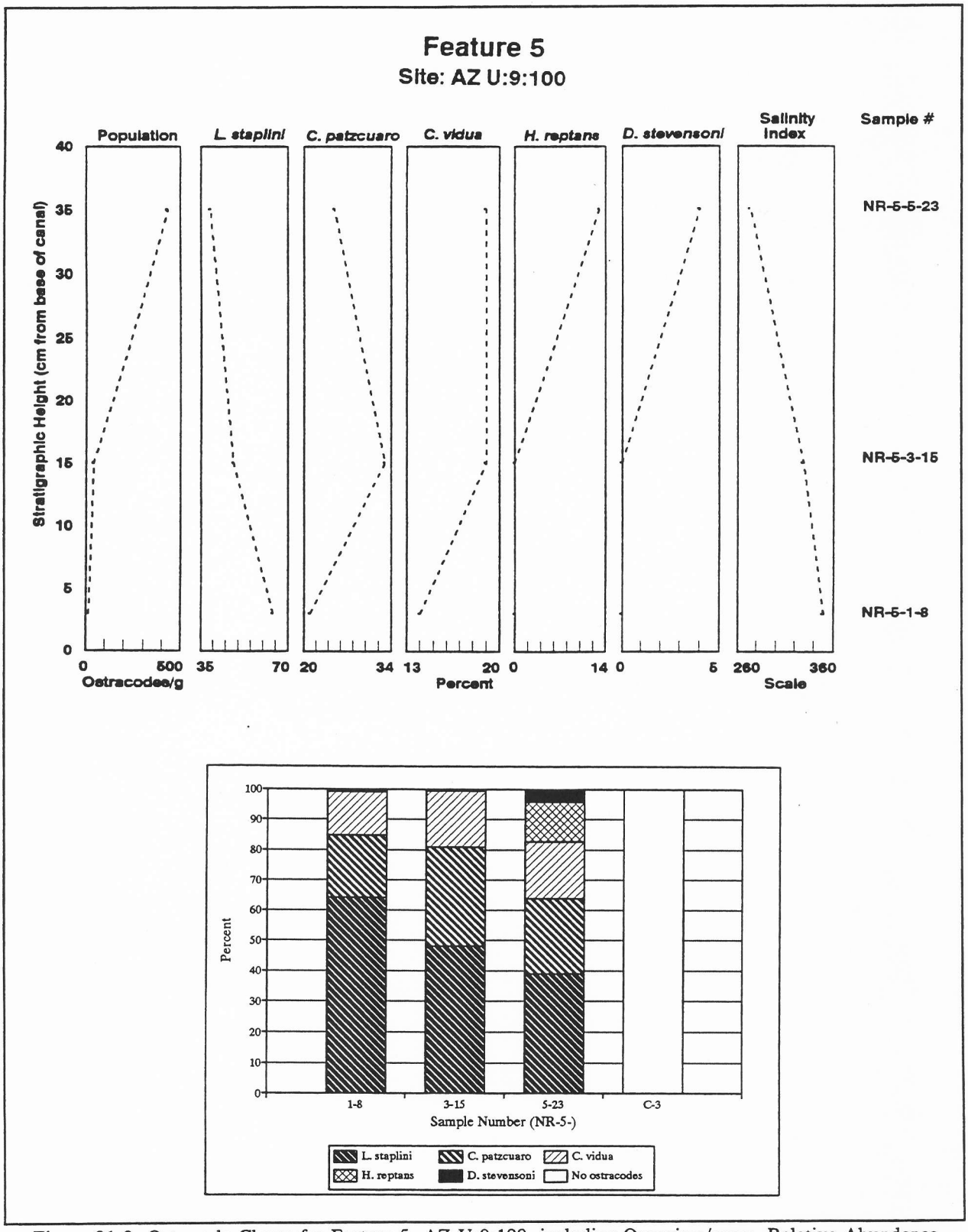

Figure 21.2 Ostracode Charts for Feature 5, AZ U:9:100, including Organism/gram, Relative Abundance by Species, Salinity Index, and Bar Chart of Relative Species Distribution.

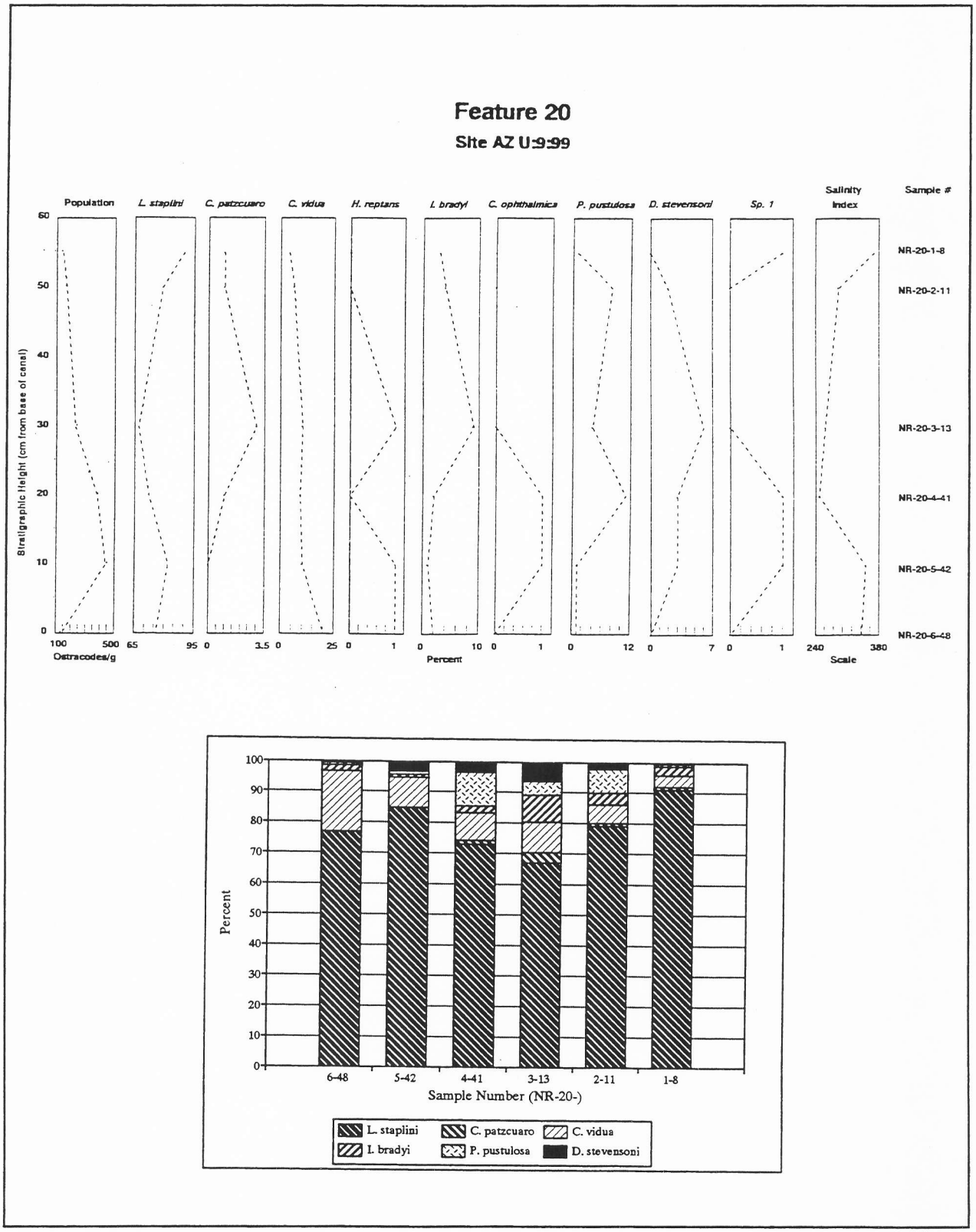

Figure 21.3 Ostracode Charts for Feature 20, AZ U:9:99, including Organism/gram, Relative Abundance by Species, Salinity Index, and Bar Chart of Relative Species Distribution.

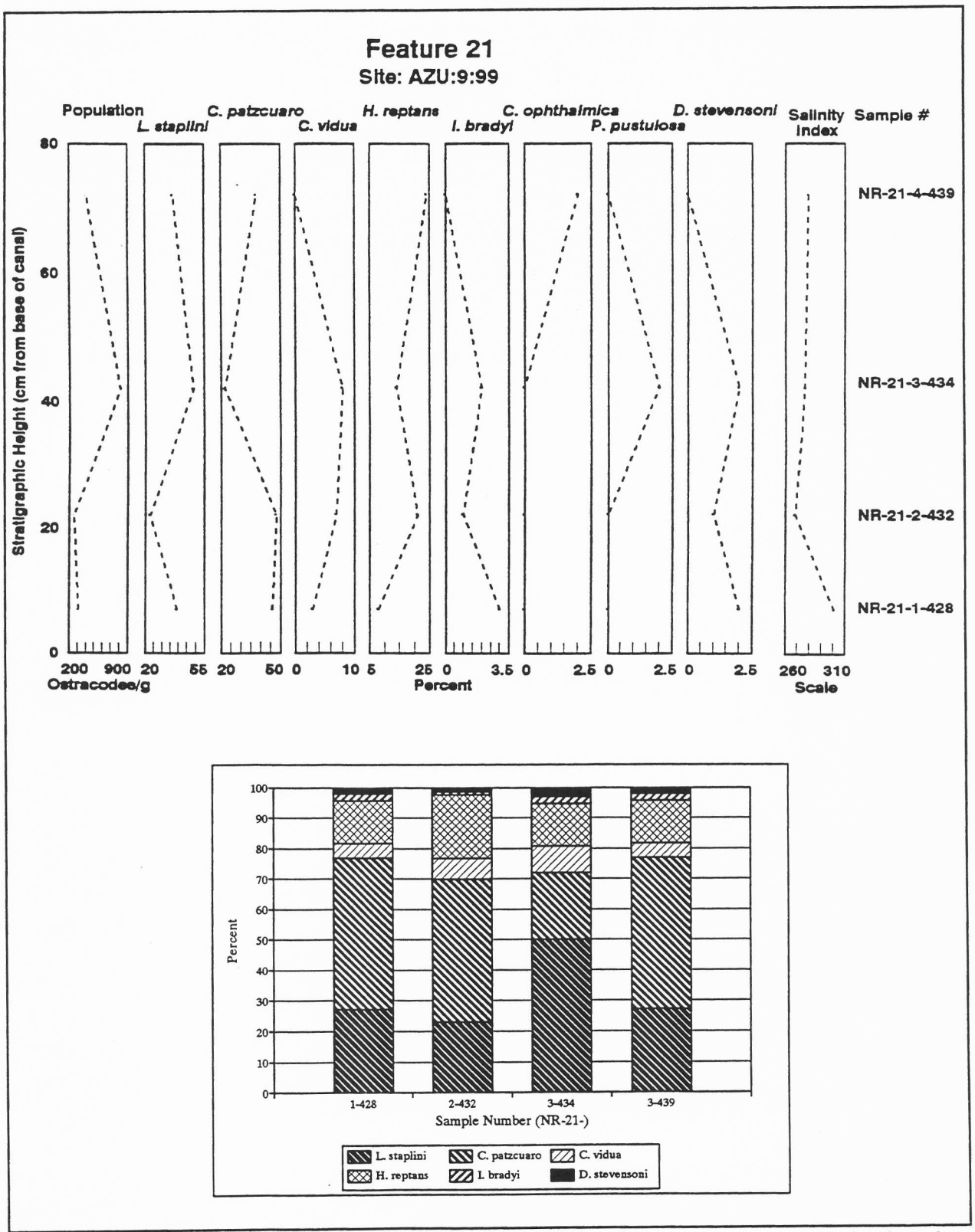

Figure 21.4 Ostracode Charts for Feature 21, AZ U:9:99, including Organism/gram, Relative Abundance by Species, Salinity Index, and Bar Chart of Relative Species Distribution.

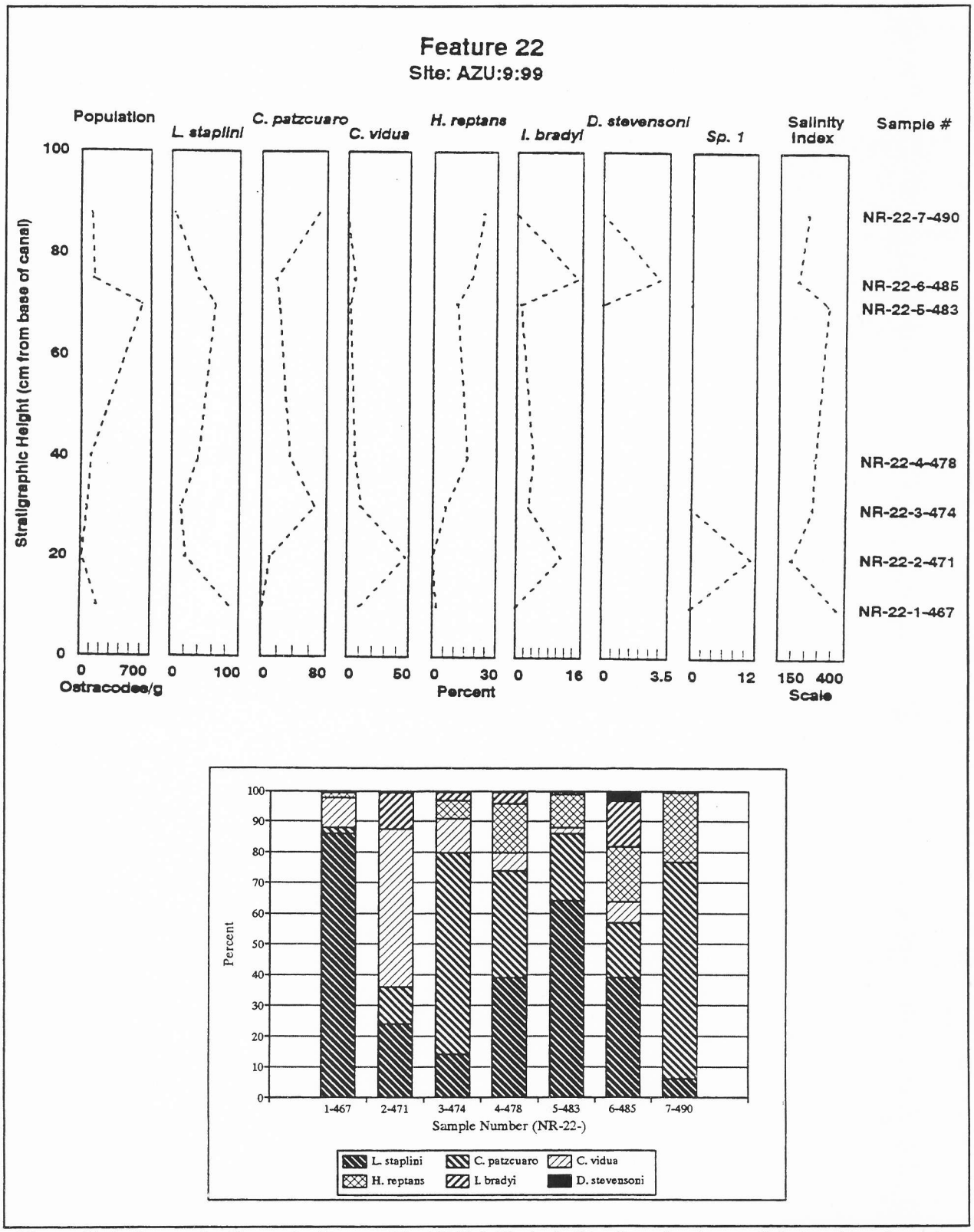

Figure 21.5 Ostracode Charts for Feature 22, AZ U:9:99, including Organism/gram, Relative Abundance by Species, Salinity Index, and Bar Chart of Relative Species Distribution.

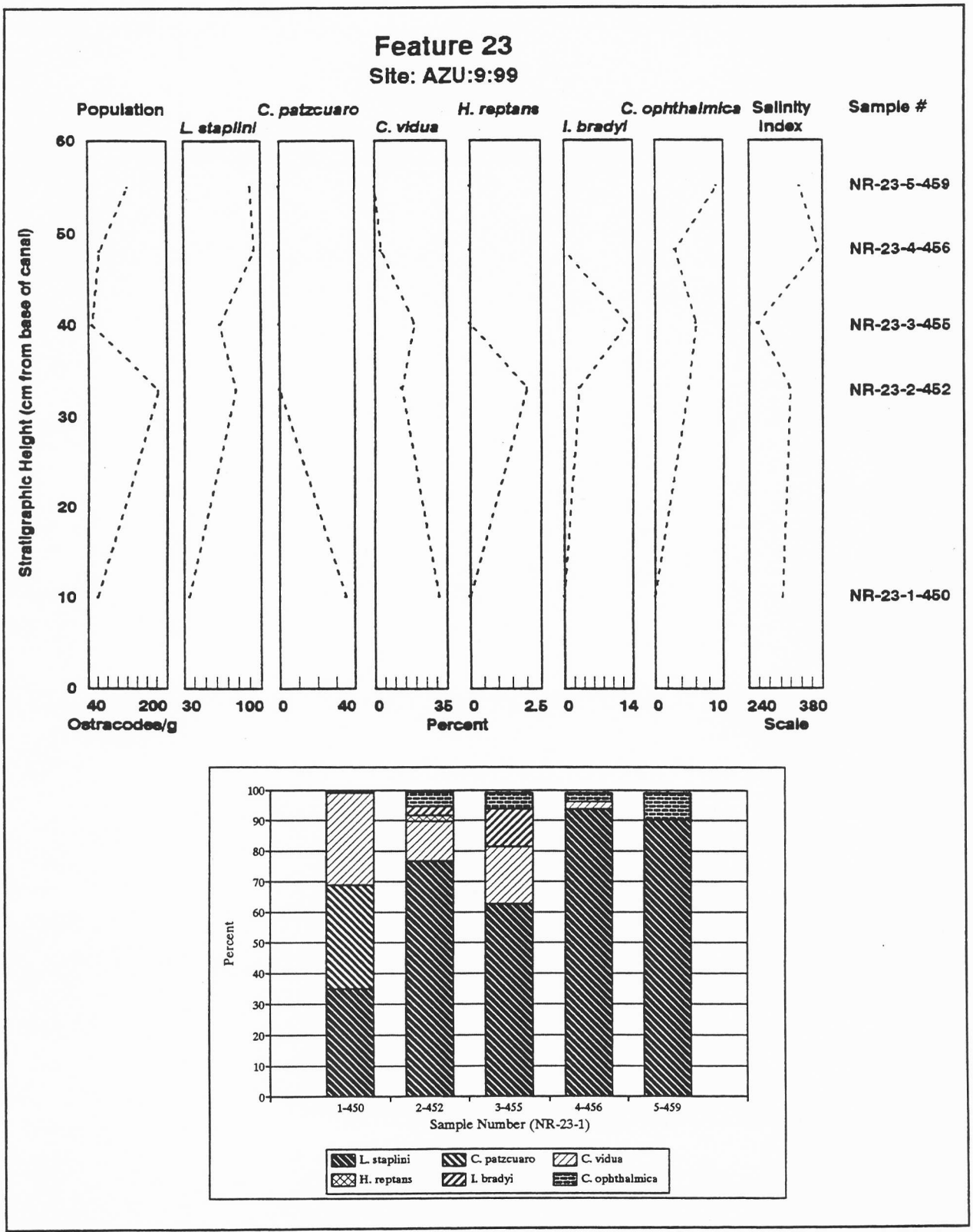

Figure 21.6 Ostracode Charts for Feature 23, AZ U:9:99, including Organism/gram, Relative Abundance by Species, Salinity Index, and Bar Chart of Relative Species Distribution.

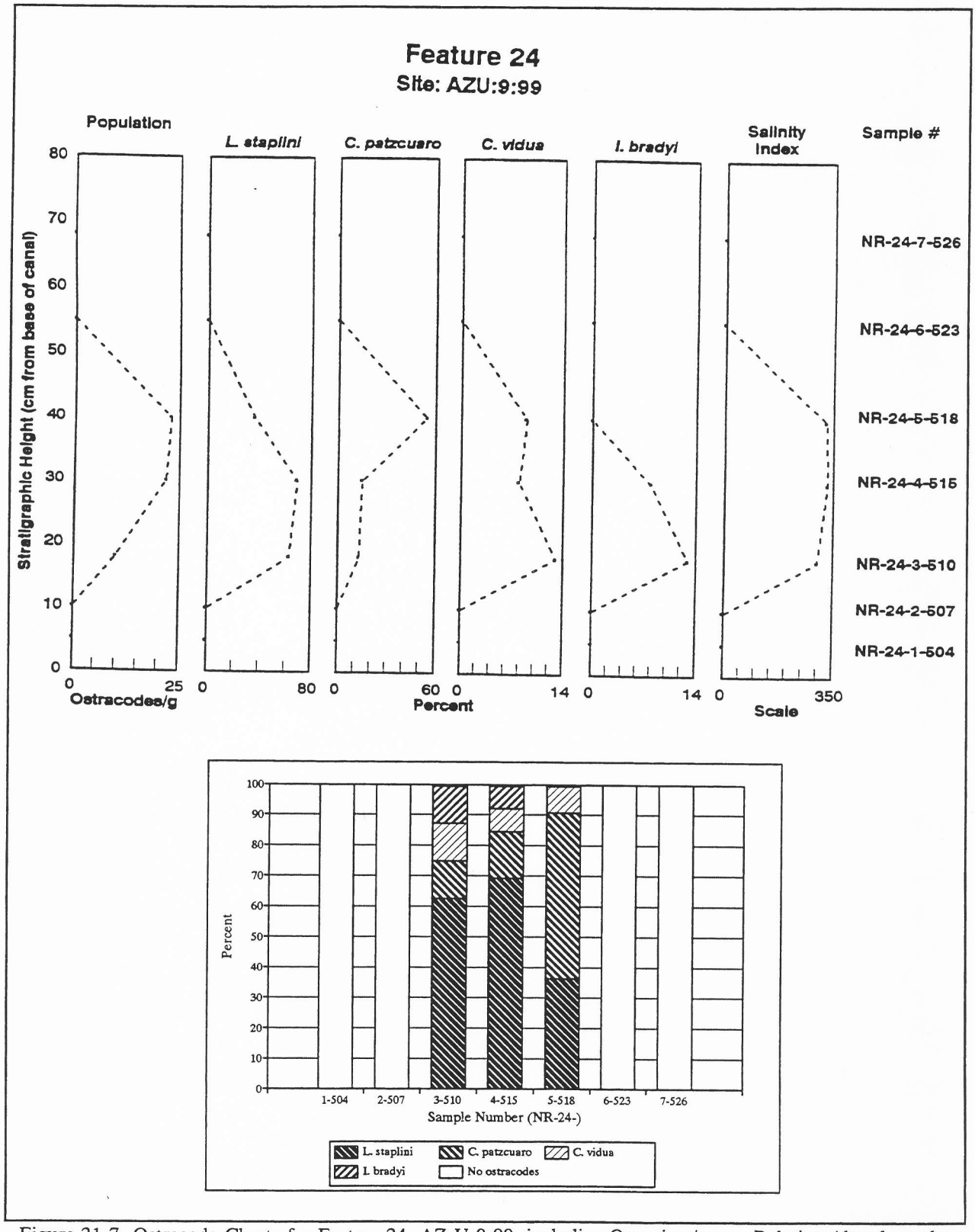

Figure 21.7 Ostracode Charts for Feature 24, AZ U:9:99, including Organism/gram, Relative Abundance by Species, Salinity Index, and Bar Chart of Relative Species Distribution.

Figure 21.5 summarizes the species occurrence patterns in Feature 22. Seven species were present in this canal, including the unidentified Sp. 1. Note that this unidentified species occurred with only one other canal (Feature 20), but the colony was not as abundant as it was in Feature 22. Total population varied widely between samples. The relative abundance charts suggest that a few species occurred occasionally (*D. stevensoni* and Sp. 1), but all others were more consistent and well represented. The paleosalinity index reflects this diverse fauna. The bar chart shows the proportional frequency of each species per sample; three assemblages characterized this canal. At the beginning of the record, assemblage I (*L. staplini*-dominated) entered the system but rapidly evolved into assemblage IV (*C. vidua*-dominated). This is the only case in which this assemblage was recognized. Subsequently, it changed to assemblage III (*C. patzcuaro*-dominated), then to assemblage I, and finally returned to assemblage III.

Figure 21.6 illustrates the canal history of Feature 23. The total population chart shows a moderate abundance of carapaces. Six species occurred in this feature. The paleosalinity index and the bar chart clearly show *L. staplini*'s dominance. Feature 23 varied from assemblage II (near-equivalent proportions of *L. staplini-C. patzcuaro-C. vidua*) to assemblage I (*L. staplini*-dominated).

Figure 21.7 presents the species occurrence patterns of Feature 24. The total population chart shows the lowest population of all seven canals; four species occurred in this canal, but at low levels. The relative abundance charts indicate that *L. staplini* and *C. patzcuaro* were the dominant species. The paleosalinity index is controlled by *L. staplini*, but *C. patzcuaro* and, to a lesser extent, *C. vidua* influences the curve's trend. The initial uses of the canal had no ostracodes. The middle uses of the canal included evidence of assemblage I and assemblage III. The disappearance of ostracodes from this canal was as abrupt as their appearance.

Trace Element Data

Shell chemistry information, obtained from 158 individual valves of *Limnocythere staplini* collected from seven canal features, provides a means by which the condition of water in the canals at the time of deposition can be established. The geochemical data is summarized in Tables 21.5–21.11. For each canal feature, the tables list the stratigraphic position of each sample from the base of the canal, the sample number, number of replicates (valves analyzed per interval), ^{m}(Mg/Ca) and ^{m}(Sr/Ca) molar ratios, and average temperature and salinity (per interval). Additional geochemical data used in the derivation of the molar ratios is provided in Appendix Q. Figures 21.8–21.14 plot the ^{m}(Mg/Ca) and ^{m}(Sr/Ca) molar ratios from ostracode valves and the temperature (°C) and salinity (TDS in ppm) estimates. The paleosalinity index derived from ostracode occurrence is provided for comparative purposes. Temperature and salinity approximations were obtained using experimentally derived multiple regression constants (Palacios-Fest 1994b).

Alternating conditions are consistent with the evaporative events that must have affected Hohokam irrigation systems. Tight clusters of ^{m}(Mg/Ca) and ^{m}(Sr/Ca) ratios indicate small temperature and/or salinity variations. Short fluctuations are more likely to occur in a permanent (or long-term) water body, whereas broad fluctuations of geochemical values imply the variable conditions more often seen under evaporative (or short-term) conditions. Temperature and salinity estimates generally track the trace element trends. However, they sometimes show a more intense change, suggesting that a small fluctuation in the trace element ratio may reflect a more acute environmental variation. Hence, temperature and salinity graphs were plotted separately.

Trace element ratios and paleoenvironmental estimates of individual carapaces from Feature 1 are shown in Table 21.5 and Figure 21.8. Of the 32 carapaces examined from Feature 1, the maximum ^{m}(Mg/Ca) ratios range from .0042 to .0109. The sample or interval NR-1-6-48 shows the greatest variation (.0044–.0109), whereas several intervals (NR-1-7-53, NR-1-12-73, NR-1-15-88) show clustered data (Figure 21.8a). Within this feature, ^{m}(Sr/Ca) ratios range from .00031 to .00122. Again, NR-1-6-48 shows the greatest variation (.0031–.00122), and NR-1-7-53, NR-1-12-73 and NR-1-15-88 are tightly clustered (Figure 21.8c). Using equation (1), temperature estimates indicate that the canal water fluctuated from 5° to 14° C during the feature's operation (Figure 21.8b). Intervals NR-1-6-48 and NR-1-15-88 show sharper positive peaks than the ^{m}(Mg/Ca) ratio trends, probably small changes in these ratios indicate that a small amount of Mg^{2+} was required with increasing temperature.

Fluctuations were also documented in the average salinity estimates obtained using equation (2); the salinity estimates ranged broadly from 1,771 to 3,831

Table 21.5. *Limnocythere staplini* Trace Element Data for Feature 1, including Mg/Ca and Sr/Ca Molar Ratios, Temperature Estimates, and Salinity Estimates.

Stratigraphic Position from Canal Base (cm)	Sample	Replicate	^{m}(Mg/Ca)	^{m}(Sr/Ca)	Temperature Estimate (°C)	Average Temperature (°C)	Salinity Estimate (TDS=ppm)	Average Salinity (TDS=ppm)
15	NR-1-1	A	.0083	.00049	10	8	2,123	2,063
		B	.0074	.00067	9		3,008	
		C	.0051	.00036	6		1,434	
		D	.0047	.00041	5		1,686	
35	NR-1-3	A	.0063	.00031	7	6	1,209	1,771
		B	.0053	.00057	6		2,524	
		C	.0043	.00038	5		1,537	
		D	.0050	.00043	6		1,815	
65	NR-1-6	A	.0109	.00122	14	10	5,773	3,831
		B	.0097	.00098	12		4,527	
		C	.0058	.00074	7		3,333	
		D	.0044	.00047	5		2,020	
		E	.0087	.00077	11		3,501	
75	NR-1-7	A	.0064	.00056	8	8	2,462	2,768
		B	.0069	.00080	8		3,653	
		C	.0074	.00059	9		2,580	
		D	.0061	.00054	7		2,338	
		E	.0075	.00063	9		2,805	
95	NR-1-9	A	.0053	.00031	6	7	1,178	1,819
		C	.0042	.00046	5		1,930	
		D	.0064	.00054	8		2,345	
		E	.0065	.00043	8		1,824	
125	NR-1-12	A	.0049	.00046	5	6	1,935	2,185
		B	.0057	.00068	7		3,044	
		C	.0052	.00049	6		2,099	
		D	.0060	.00044	7		1,846	
		E	.0061	.00047	7		2,004	
155	NR-1-15	A	.0068	.00057	8	9	2,522	2,344
		B	.0084	.00068	10		3,034	
		C	.0071	.00049	9		2,102	
		D	.0069	.00045	8		1,890	
		E	.0077	.00050	9		2,172	

ppm of TDS in Feature 1. In contrast with the temperature plot, however, the salinity trend shows an acute increase in salinity at sample NR-1-6-48. Other samples remain at approximately the same TDS concentration (Figure 21.8d).

A comparison between the trace element estimated salinity and the paleoecologically derived paleosalinity index of Feature 1 shows a close correlation for the stratigraphic samples between NR-1-3-37 and NR-1-9-61. A minor difference is observed between samples NR-1-1-28 and NR-1-3-37, at the bottom of the canal. However, there is a drastic change in salinity based on ostracode occurrence between NR-1-9-61 and NR-1-12-73 that is not shown by the ^{m}(Sr/Ca) ratio. It is possible that apparent water freshening, indicated by the paleosalinity index, was due to water input stabilization. Water stability would allow more species to occur; canal flooding or regrading improvements may have introduced new species to the system (Figure 21.8e).

Trace element data and paleoenvironmental estimates for Feature 5 are presented in Table 21.6 and

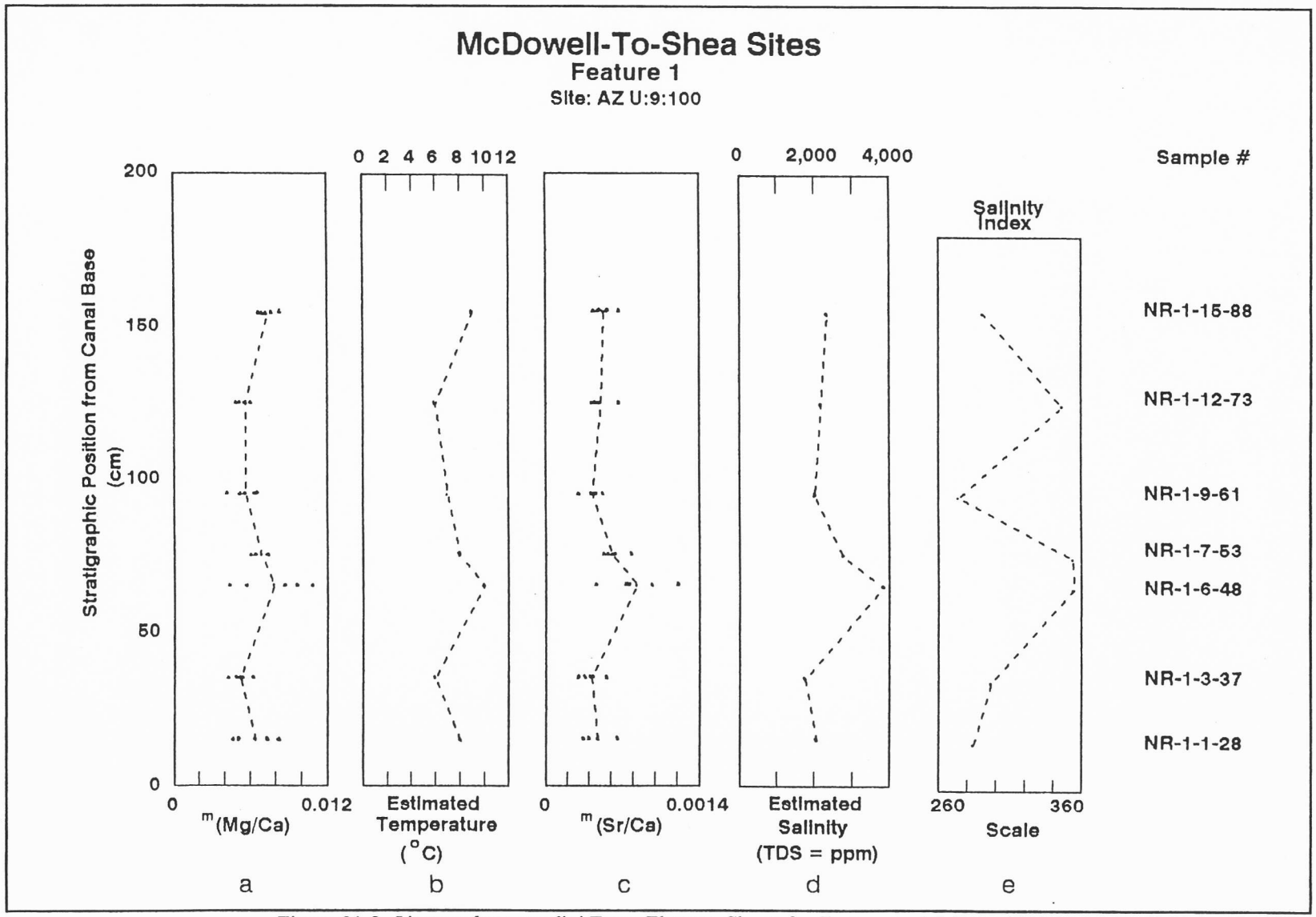

Figure 21.8 *Limnocythere staplini* Trace Element Charts for Feature 1, AZ U:9:100.

Table 21.6. *Limnocythere staplini* Trace Element Data for Feature 5, including Mg/Ca and Sr/Ca Molar Ratios, Temperature Estimates, and Salinity Estimates.

Stratigraphic Position from Canal Base (cm)	Sample	Replicate	^{m}(Mg/Ca)	^{m}(Sr/Ca)	Temperature Estimate (°C)	Average Temperature (°C)	Salinity Estimate (TDS=ppm)	Average Salinity (TDS=ppm)
3	NR-5-1	A	.0080	.00050	10	8	2,172	2,766
		B	.0052	.00059	6		2,619	
		C	.0056	.00054	6		2,338	
		D	.0098	.00090	12		4,173	
		E	.0066	.00058	8		2,530	
15	NR-5-3	A	.0046	.00033	5	7	1,308	1,563
		B	.0047	.00043	5		1,790	
		C	.0067	.00033	8		1,291	
		D	.0088	.00033	11		1,316	
		E	.0055	.00049	6		2,109	
35	NR-5-5	A	.0052	.00057	6	8	2,493	1,962
		B	.0073	.00069	9		3,124	
		C	.0065	.00024	8		859	
		D	.0066	.00034	8		1,373	

Figure 21.9. The maximum ^{m}(Mg/Ca) ratios between carapaces from one stratum range from .0046 to .0088. Interval NR-5-5-23, from the highest stratum in the canal, shows tightly clustered values (.0055–.0073), whereas the other two intervals indicate broad fluctuations in Mg^{2+} uptake (Figure 21.9a).

Among the strata of Feature 5, the ^{m}(Sr/Ca) ratios range from .00033 to .00090. Sample NR-5-3-15 from the middle strata shows clustered values, whereas sample NR-5-5-23 has the broadest variation in trace element ratios (Figure 21.9c).

Temperature estimates show almost no variation during canal use (7°–8° C), suggesting a consistent operation (Figure 21.9b). Estimates of salinity (1,563–2,766 ppm) are more variable than the temperature estimates, which suggests stable conditions but increasing salinization after canal flooding or regrading improvements (Figure 21.9d). The apparent difference between geochemical salinity trends and the paleosalinity index may correspond to the abrupt appearance of species at the end of the record (Figure 21.9e). Species occurrence may be due to canal water stagnation.

Trace element and paleoenvironmental records of Feature 20 are shown in Table 21.7 and Figure 21.10. The maximum ^{m}(Mg/Ca) ratios range from .0037 to .0199. Intervals NR-20-1-8 and NR-20-2-11, the uppermost stratum samples in the canal, show the broadest trace element variations. The remaining samples' values are tightly clustered (Figure 21.10a).

The ^{m}(Sr/Ca) ratios of Feature 20 follow a similar pattern with values ranging from .00030 to .00153 in the two upper strata (Figure 21.10c). Lower elevations of the canal have more consistent values.

Temperature estimates from Feature 20 suggest a gradual increase from 7° to 13° C through time (Figure 21.10b). Salinity estimates range from 2,720 to 5,038 ppm (Figure 21.10d). They show almost no change throughout the canal's history, except near the end of the record. The paleosalinity index and the geochemical salinity plot are consistent, although an apparent low salinity record is registered at sample NR-20-4-41. It is possible that this discrepancy results from canal stabilization, which allowed the growth of several ostracode species (Figure 21.10e).

The geochemical and paleoenvironmental data of Feature 21 are shown in Table 21.8 and Figure 21.11. In this feature, the ^{m}(Mg/Ca) ratios range from .0040 to .0085. Interval NR-21-4-439 has the tightest cluster of values, whereas the remaining samples show wide fluctuations (Figure 21.11a). Sample NR-21-2-432, near the base of the canal, has the largest variability (.0054–.0085).

The ^{m}(Sr/Ca) ratios from Feature 21 range from .00023 to .00074. Consistent with the pattern shown by the ^{m}(Mg/Ca) ratios, the upper stratum sample NR-21-4-439 has the tightest cluster of values, while sample NR-21-2-432, near the lower canal levels, shows the broadest fluctuations in strontium ratios: .00042–.00074 (Figure 21.11c).

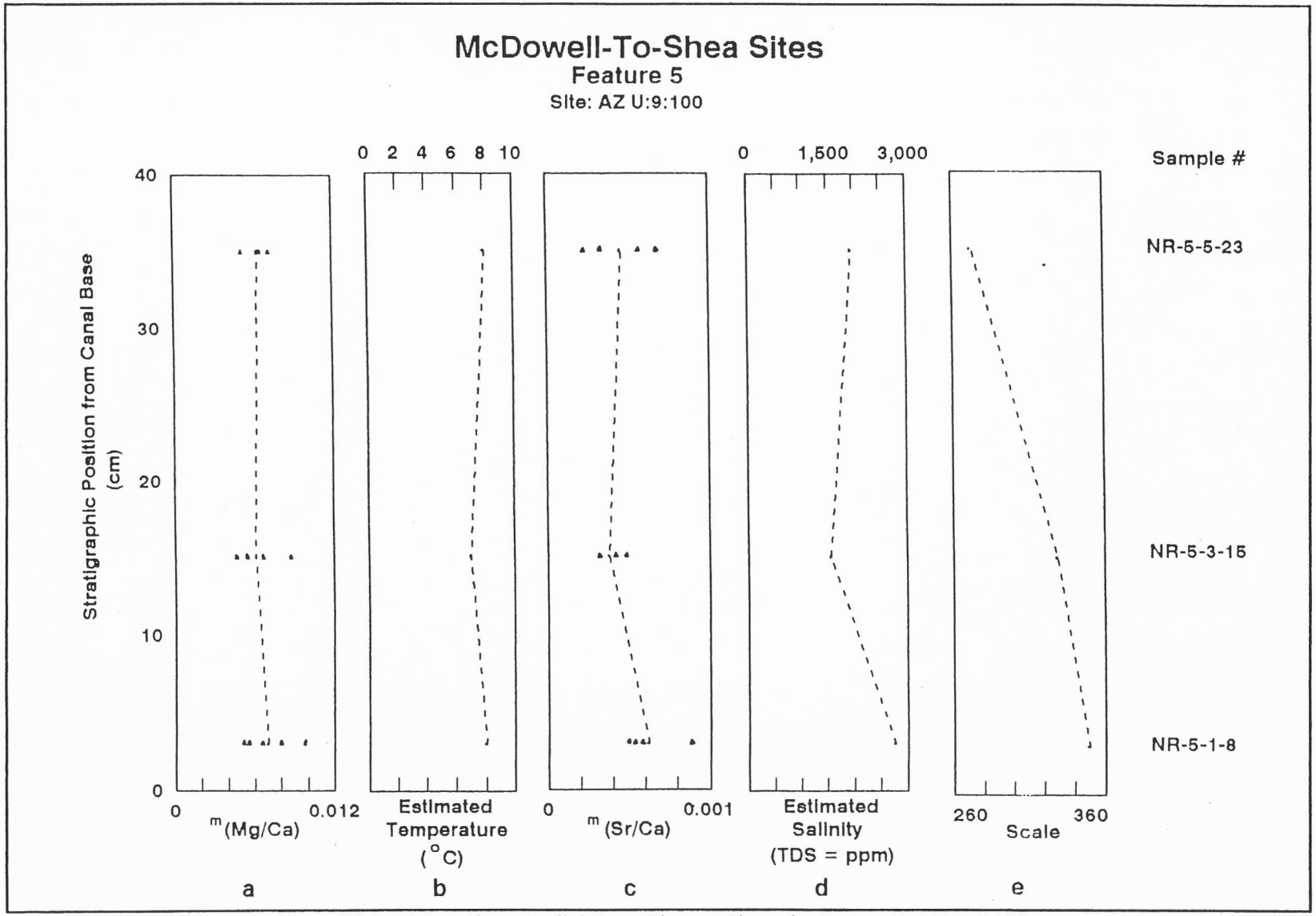

Figure 21.9 *Limnocythere staplini* Trace Element Charts for Feature 5, AZ U:9:100.

Table 21.7. *Limnocythere staplini* Trace Element Data for Feature 20, including Mg/Ca and Sr/Ca Molar Ratios, Temperature Estimates, and Salinity Estimates.

Stratigraphic Position from Canal Base (cm)	Sample	Replicate	^{m}(Mg/Ca)	^{m}(Sr/Ca)	Temperature Estimate (°C)	Average Temperature (°C)	Salinity Estimate (TDS=ppm)	Average Salinity (TDS=ppm)
55	NR-20-1	A	.0081	.00092	10	13	4,258	5,038
		B	.0199	.00153	26		7,317	
		C	.0121	.00140	15		6,657	
		D	.0061	.00088	7		4,036	
		E	.0064	.00065	8		2,920	
50	NR-20-2	A	.0152	.00151	19	10	7,185	3,825
		B	.0037	.00030	4		1,153	
		C	.0057	.00068	7		3,043	
		D	.0084	.00099	10		4,619	
		E	.0074	.00069	9		3,122	
30	NR-20-3	A	.0061	.00062	7	7	2,733	3,058
		B	.0065	.00070	8		3,155	
		C	.0072	.00085	9		3,895	
		D	.0051	.00056	6		2,449	
20	NR-20-4	A	.0064	.00073	8	7	3,308	3,084
		B	.0052	.00062	6		2,728	
		C	.0050	.00067	6		3,003	
		D	.0062	.00073	7		3,295	
10	NR-20-5	A	.0092	.00055	11	9	2,385	2,720
		B	.0059	.00059	7		2,623	
		C	.0064	.00055	8		2,381	
		D	.0077	.00077	9		3,489	
0	N4-20-6	A	.0070	.00067	8	7	3,001	2,858
		B	.0053	.00058	6		2,552	
		C	.0064	.00065	7		2,881	
		D	.0064	.00067	7		2,998	

Temperature estimates indicate low values (5°–8° C) throughout the canal record (Figure 21.11b). Salinity estimates show low concentrations (1,148–2,537 ppm), which abruptly increase at interval NR-21-2-432 (Figure 21.11d). In contrast, the paleosalinity index generates a mirror image of the trace element salinity (Figure 21.11e). Although the ^{m}(Sr/Ca) ratios suggest a sharp increase in salinity followed by a gradual decrease of this parameter, the paleoecologic record indicates just the opposite; the relationship between these trends is controversial and unclear.

Table 21.9 and Figure 21.12 show the trace element and paleoenvironmental records from Feature 22. Among strata, the ^{m}(Mg/Ca) ratios range from .0042 to .0170 (Figure 21.12a), and the ^{m}(Sr/Ca) ratios range from .00015 to .00128 (Figure 21.12c). Most of the intervals show broad fluctuations in trace element values for the two ratios, suggesting that this canal was continuously subject to evaporitic conditions. Temperature estimates from the feature have the highest values (9°–15° C) recorded from all canals, but these gradually decrease toward the end of the record (Figure 21.12b). Salinity estimates show high salt concentration (1,870–4,529 ppm) in the lower strata of the canal, which slowly decreases toward the upper levels (Figure 21.12d). A comparison between this trend and the paleosalinity index (Figure 21.12e) shows a congruent trend (from sample NR-22-1-467 to NR-22-3-478), but an inconsistent and unclear behavior in the upper samples.

Feature 23's geochemical and paleoenvironmental data are presented in Table 21.10 and Figure 21.13. The ^{m}(Mg/Ca) ratios for the sampled strata in the feature range from .0052 to .0110. NR-23-4-456 and

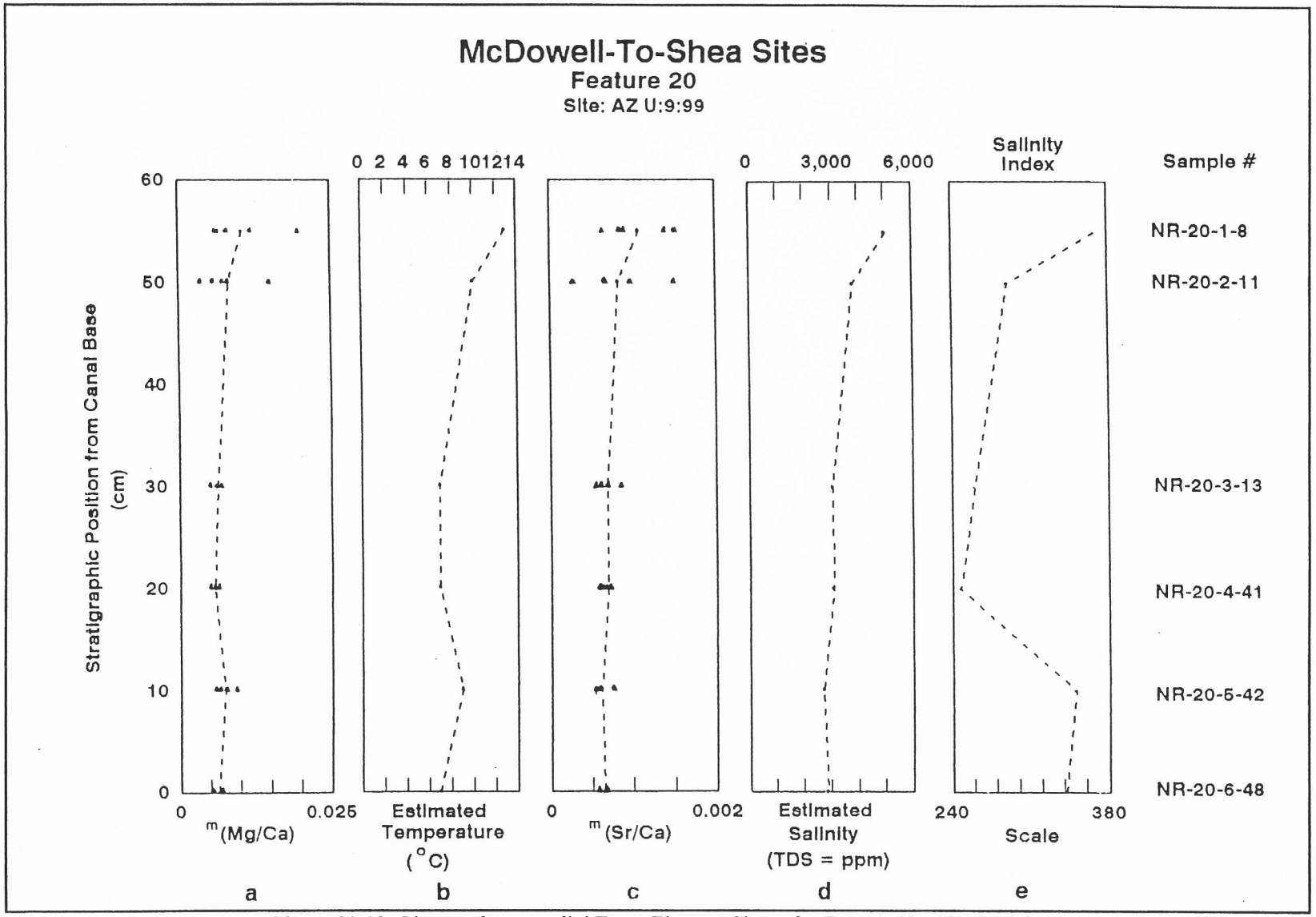

Figure 21.10 *Limnocythere staplini* Trace Element Charts for Feature 20, AZ U:9:99.

Table 21.8. *Limnocythere staplini* Trace Element Data for Feature 21, including Mg/Ca and Sr/Ca Molar Ratios, Temperature Estimates, and Salinity Estimates.

Stratigraphic Position from Canal Base (cm)	Sample	Replicate	^{m}(Mg/Ca)	^{m}(Sr/Ca)	Temperature Estimate (°C)	Average Temperature (°C)	Salinity Estimate (TDS=ppm)	Average Salinity (TDS=ppm)
7	NR-21-1	A	.0064	.00037	8	6	1,490	1,630
		B	.0062	.00031	7		1,200	
		C	.0042	.00054	5		2,334	
		D	.0041	.00035	4		1,397	
		E	.0056	.00042	6		1,728	
22	NR-21-2	A	.0068	.00066	8	8	2,929	2,537
		B	.0054	.00056	6		2,451	
		C	.0055	.00074	6		3,342	
		D	.0085	.00051	10		2,218	
		E	.0074	.00042	9		1,746	
42	NR-21-3	A	.0064	.00048	8	6	2,030	1,765
		B	.0057	.00049	7		2,120	
		C	.0052	.00031	6		1,210	
		D	.0044	.00043	5		1,797	
		E	.0050	.00040	6		1,667	
72	NR-21-4	A	.0048	.00035	5	5	1,393	1,148
		B	.0045	.00028	5		1,066	
		C	.0046	.00023	5		790	
		D	.0040	.00030	4		1,146	
		E	.0044	.00034	5		1,345	

NR-23-5-459, from the highest sampled levels of the feature, show tightly clustered values, whereas other samples indicate broad fluctuations in Mg^{2+} content (Figure 21.13a).

The ^{m}(Sr/Ca) ratios range from .00049 to .00091. Of note, these extremes were recorded from carapaces in the same stratigraphic unit. Samples NR-23-1-450 and NR-23-5-459 show the closest measurements of Sr^{2+} values, even though they were collected from the highest and lowest strata in the canal. In contrast, other samples show broad fluctuations in Sr^{2+} content (Figure 21.13c), but with a mean determination that varies only slightly from the high and low sample.

Temperature estimates indicate decreasing values from 11° to 7° C (Figure 21.13b), whereas the salinity estimates (Figure 21.13d) show no significant variation throughout the canal's history (2,997–3,500 ppm). In contrast with the paleosalinity index, the ^{m}(Sr/Ca) data indicate that this canal was consistently saline. The apparent discrepancy between these two trends probably resulted from the stabilization of the canal after flooding, allowing ostracode species to populate it. Canal use when sample NR-23-3-455 was deposited introduced some species to the system, but its hostile environment encouraged a return to previous conditions (Figure 21.13e).

The trace element and paleoenvironmental records from Feature 24 are shown in Table 21.11 and Figure 21.14. The maximum ^{m}(Mg/Ca) ratios range from .0052 to .0143 between stratigraphic units. Feature 24's sample NR-24-4-515 has the broadest fluctuations in Mg^{2+} content, whereas the remaining two samples show tight clusters (Figure 21.14a). The ^{m}(Sr/Ca) ratios range from .00018 to .00079. Sample NR-24-3-510 exhibits the tightest clustering of results; the other two samples from this canal show widely variable values (Figure 21.14c).

Temperature estimates vary from 7° to 11° C; the earlier canal use had a lower temperature than the late part of the canal's history (Figure 21.14b). Salinity estimates range from 1,635 to 2,648 ppm (Figure 21.14d). The paleosalinity index (Figure 21.14e) and the estimated salinity curves are somewhat consistent since both suggest that this canal ranged from moderately to highly saline. However, the sharp increase in salinity shown by the salinity curve is not evident in the

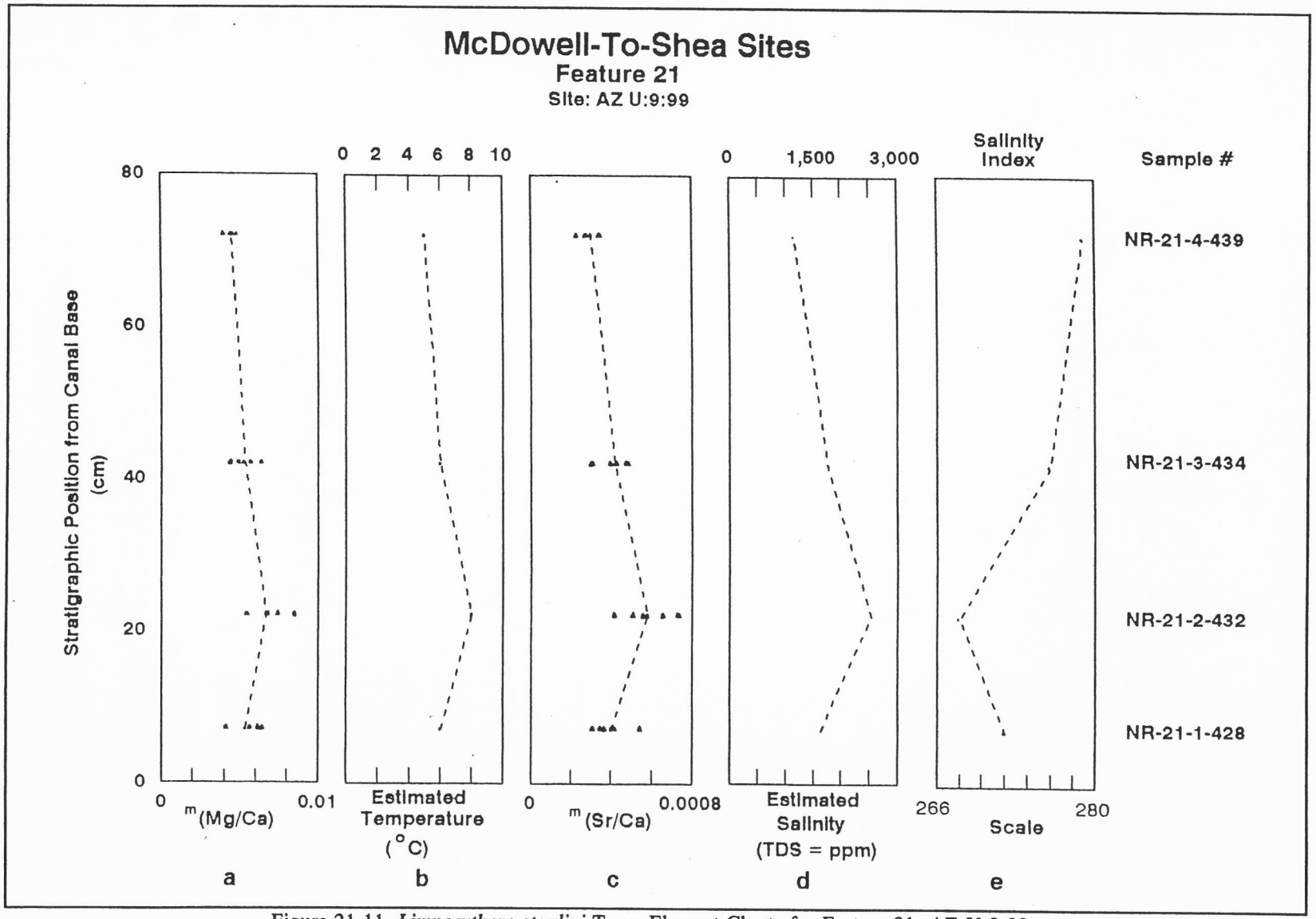

Figure 21.11 *Limnocythere staplini* Trace Element Charts for Feature 21, AZ U:9:99.

Table 21.9. *Limnocythere staplini* Trace Element Data for Feature 22, including Mg/Ca and Sr/Ca Molar Ratios, Temperature Estimates, and Salinity Estimates.

Stratigraphic Position from Canal Base (cm)	Sample	Replicate	^{m}(Mg/Ca)	^{m}(Sr/Ca)	Temperature Estimate (°C)	Average Temperature (°C)	Salinity Estimate (TDS=ppm)	Average Salinity (TDS=ppm)
10	NR-22-1	A	.0102	.00075	13	15	3,404	4,100
		B	.0102	.00091	13		4,195	
		C	.0097	.00089	12		4,103	
		D	.0163	.00077	21		3,507	
		E	.0129	.00113	16		5,291	
20	NR-22-2	A	.0080	.00033	10	14	1,302	3,343
		B	.0168	.00128	22		6,052	
		C	.0102	.00058	13		2,537	
		D	.0103	.00077	13		3,480	
30	NR-22-3	A	.0086	.00083	11	14	3,807	4,529
		B	.0094	.00113	12		5,313	
		C	.0102	.00098	13		4,574	
		D	.0170	.00106	22		4,935	
		E	.0093	.00087	11		4,016	
40	NR-22-4	A	.0069	.00081	8	8	3,704	2,719
		B	.0062	.00060	7		2,652	
		C	.0093	.00039	11		1,597	
		D	.0047	.00059	5		2,600	
		E	.0071	.00068	9		3,044	
70	NR-22-5	A	.0079	.00072	10	10	3,251	1,870
		B	.0042	.00015	5		414	
		C	.0088	.00067	11		2,980	
		D	.0119	.00034	15		1,371	
		E	.0085	.00034	10		1,332	
75	NR-22-6	A	.0042	.00024	5	9	835	2,489
		B	.0088	.00068	11		3,061	
		C	.0080	.00063	10		2,804	
		D	.0088	.00069	11		3,099	
		E	.0077	.00060	9		2,645	

paleosalinity index probably because the latter is mostly driven by the dominance of *L. staplini*.

Interpretation

Table 21.12 summarizes the history of canal operations during the pre-Classic and Classic periods. The ostracode assemblages clearly suggest periodic water salinization and freshening during canal operation. Paleoecologic composition of the canals' ostracode assemblages allows this preliminary interpretation of canal history. In addition, trace elements from carapaces provide crucial information about water temperature and salinity allowing a determination of when these canals were used and the environmental conditions prevailing during operation. By combining ostracode paleoecology and shell chemistry it is possible to demonstrate the impact of seasonal variation on water availability and canal use.

Feature 1 was sampled from seven strata that were deposited in the 14th century A.D. Paleoecological and geochemical data obtained from these samples indicate that the canal was initially flooded with fairly saline waters (assemblage III), and remained at this concentration for some period of time (NR-1-1-28 and NR-1-3-37). Temperature estimates of 6°–8° C indicate that initial canal operation occurred sometime during the early spring. Salinity estimates suggest that water was

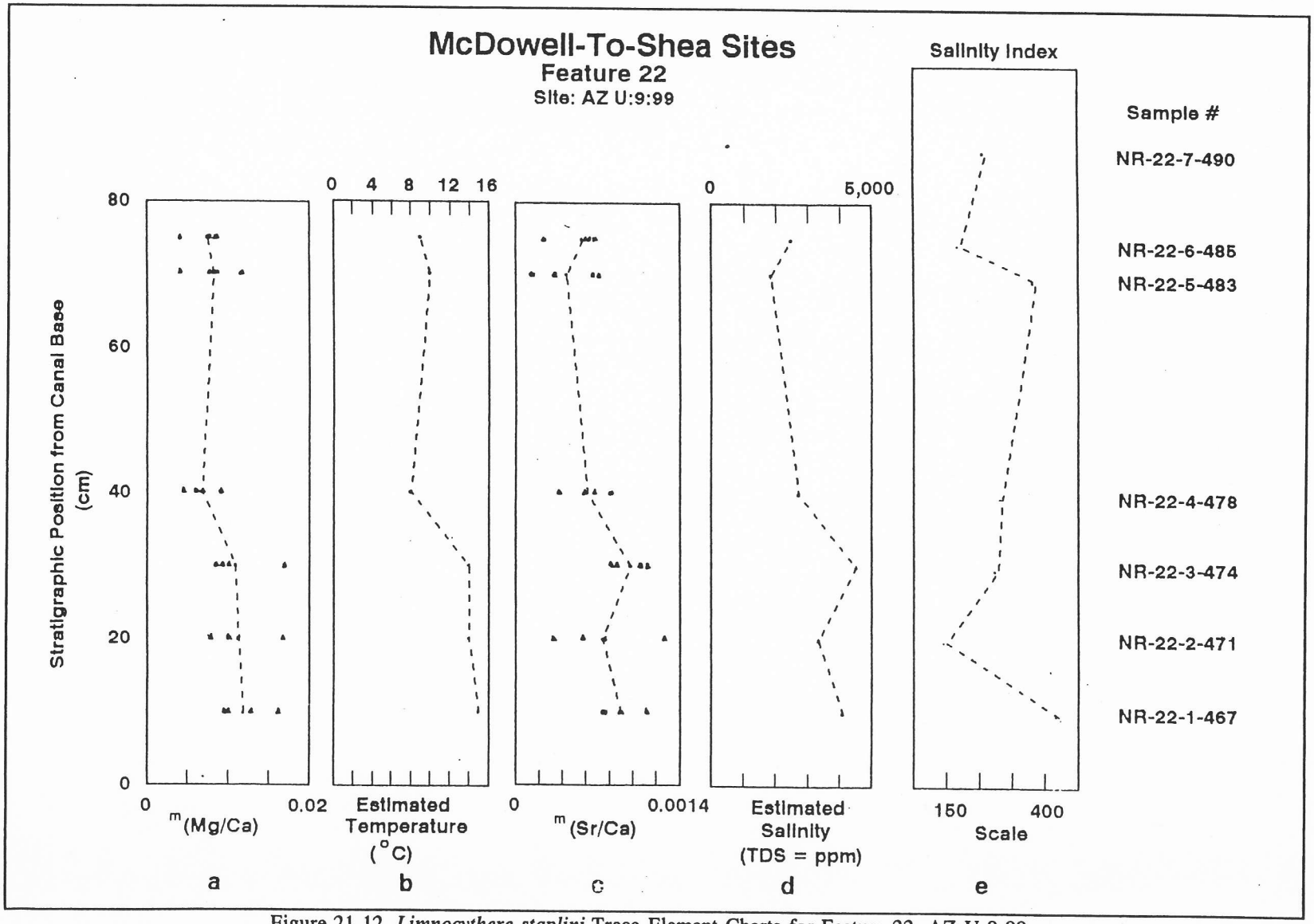

Figure 21.12 *Limnocythere staplini* Trace Element Charts for Feature 22, AZ U:9:99.

Table 21.10. *Limnocythere staplini* Trace Element Data for Feature 23, including Mg/Ca and Sr/Ca Molar Ratios, Temperature Estimates, and Salinity Estimates.

Stratigraphic Position from Canal Base (cm)	Sample	Replicate	m(Mg/Ca)	m(Sr/Ca)	Temperature Estimate (°C)	Average Temperature (°C)	Salinity Estimate (TDS=ppm)	Average Salinity (TDS=ppm)
10	NR-23-1	A	.0078	.00082	9	11	3,767	3,500
		B	.0103	.00077	13		3,512	
		C	.0091	.00068	11		3,038	
		D	.0073	.00081	9		3,682	
33	NR-23-2	A	.0110	.00049	14	11	2,124	3,331
		B	.0078	.00083	9		3,776	
		C	.0069	.00070	8		3,126	
		D	.0097	.00091	12		4,225	
		E	.0089	.00075	11		3,402	
40	NR-23-3	A	.0094	.00086	12	10	3,938	3,158
		B	.0100	.00064	12		2,851	
		C	.0082	.00085	10		3,920	
		D	.0055	.00052	6		2,261	
		E	.0073	.00063	9		2,818	
48	NR-23-4	A	.0067	.00058	8	8	2,563	2,997
		B	.0073	.00065	9		2,881	
		C	.0074	.00082	9		3,758	
		D	.0069	.00068	8		3,054	
		E	.0070	.00062	8		2,731	
55	NR-23-5	A	.0059	.00074	7	7	3,348	3,216
		B	.0068	.00075	8		3,421	
		C	.0054	.00062	6		2,747	
		D	.0052	.00074	6		3,366	
		E	.0054	.00071	6		3,196	

moderately high (1,771–2,063 ppm). However, evaporitic conditions are suggested by the appearance of assemblage I in samples NR-1-6-48 and NR-1-7-53. High salinity estimates of 2,768–3,831 ppm and the increasing estimated temperature in the range of 8°–10° C, obtained from the geochemical records, support the postulated evaporitic conditions. The latter imply agricultural activity later in the early to late spring. A "freshening" episode is characterized by assemblage III and the geochemical salinity record of 1,819–2,185 ppm. Average temperature estimates indicate cooler conditions than in the previous interval (6–7°C) as well. Although the assemblage record suggests canal salinization and refreshening, the geochemical data indicates constant conditions toward the end of the canal history. The apparent discrepancy observed in this sample is interpreted as the result of canal water stabilization which allowed several species to occur until salinity increased. This canal remained active throughout its sampled record. Episodic salinization and freshening of this canal suggest periodic water input into the system. The appearance of assemblage III (incorporating *I. bradyi* and *D. stevensoni*) in some intervals is consistent with Huckleberry's (Chapter 20) flow regime interpretation of Feature 1. Ostracode data are also consistent with low pollen records dominated by a few Cheno-Ams (Smith, Chapter 22).

Little information is available from Feature 5; three samples deposited before A.D. 1260 were analyzed. Apparently, initial flooding introduced saline water indicators (assemblage I) but continuing canal operation allowed a more stable ostracode assemblage to become established in this canal. The canal remained saline throughout its history. Low temperature estimates for this canal in the range of 7°–8° C indicate that it was mostly used during the spring or early spring. However, high salinity estimates (2,766 ppm) during the early canal operation, although consistent with the

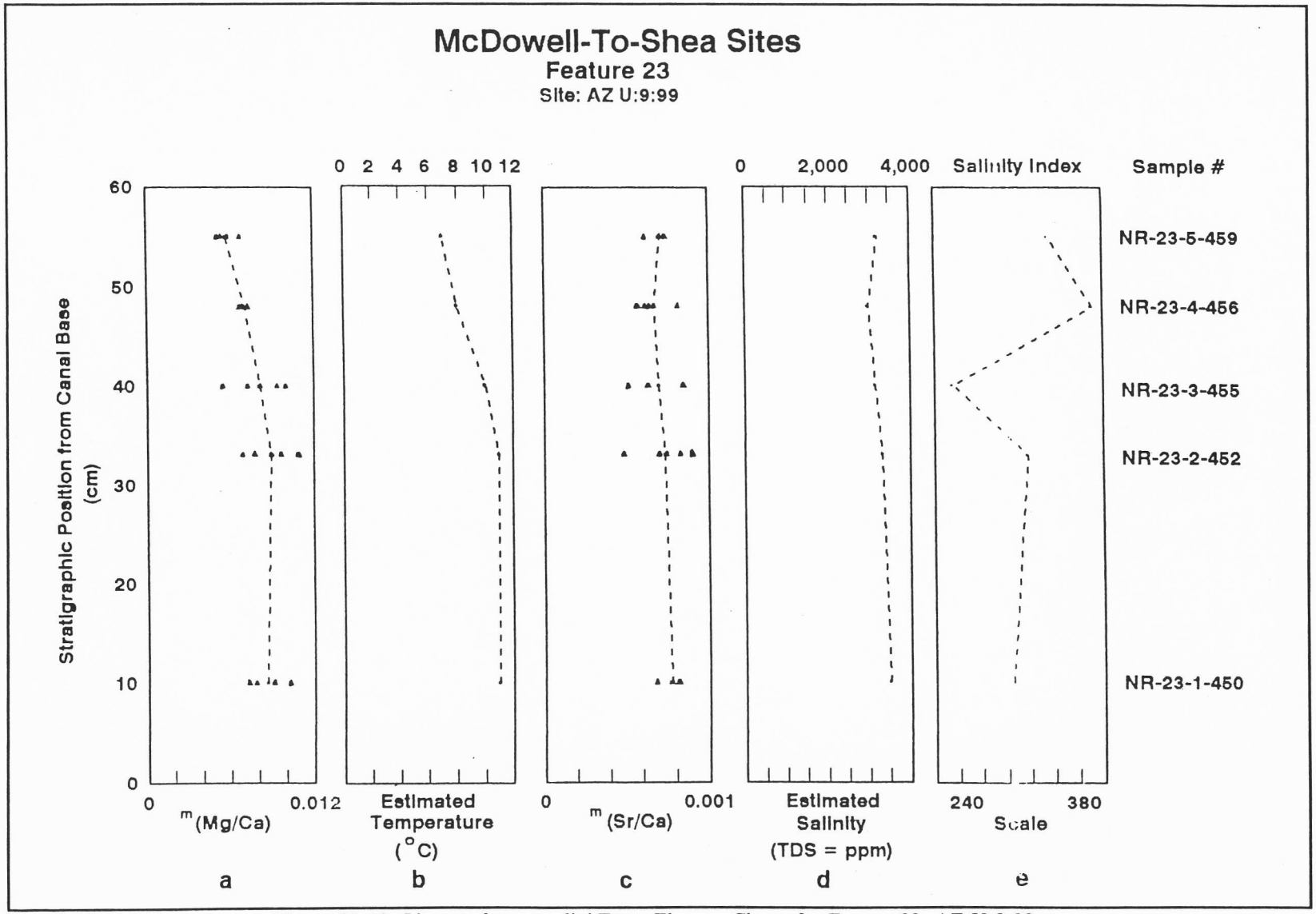

Figure 21.13 *Limnocythere staplini* Trace Element Charts for Feature 23, AZ U:9:99.

Table 21.11. *Limnocythere staplini* Trace Element Data for Feature 24, including Mg/Ca and Sr/Ca Molar Ratios, Temperature Estimates, and Salinity Estimates.

Stratigraphic Position from Canal Base (cm)	Sample	Replicate	^{m}(Mg/Ca)	^{m}(Sr/Ca)	Temperature Estimate (°C)	Average Temperature (°C)	Salinity Estimate (TDS=ppm)	Average Salinity (TDS=ppm)
18	NR-24-3	A	.0053	.00038	6	7	1,534	1,921
		B	.0052	.00058	6		2,559	
		C	.0073	.00043	9		1,803	
		D	.0066	.00043	8		1,787	
30	NR-24-4	A	.0064	.00031	8	11	1,188	1,635
		B	.0143	.00029	18		1,107	
		C	.0127	.00023	16		793	
		D	.0054	.00051	6		2,177	
		E	.0070	.00065	8		2,910	
40	NR-24-5	A	.0103	.00074	13	11	3,349	2,648
		B	.0087	.00069	11		3,118	
		C	.0081	.00018	10		538	
		D	.0099	.00079	12		3,586	

assemblage I of Feature 5, are controversial because they suggest that the canal was initially used during an evaporative period. Two possible situations may explain this discrepancy: 1) canal use occurred late in the summer, thus, ostracode data represent fall agricultural activity, or 2) canal operation began during a particularly dry winter and subsequent rainfall diluted the canal waters without a significant change in temperature. Late summer-fall canal operation is unlikely because temperature estimates are inconsistent with Phoenix Basin summer temperatures (>20°C; USDA Phoenix stations climatologic records, 1892-1990). Dry winter canal use appears a logical alternative because low temperature and high salinity are common under such conditions. Toward the end of the record salinity declined notably (almost 1,000 ppm). Salinity estimates (1,563–1,962 ppm) during the later intervals of this canal suggest gradual water dilution and a long-term water body. These variables suggest late winter to early spring conditions. Smith (Chapter 22) reports on one sample that shows increasing cattail pollen and grass, suggesting a controversial late-spring canal use.

Feature 20 was sampled from six strata. This canal was subject to flooding during an evaporative event dominated by assemblage I. The occurrence of almost all species at interval NR-20-4-41 indicates a short period of refreshening; afterwards, gradual salinization characterized this canal. Estimates of temperature (7°–13° C) and salinity (2,720–5,038 ppm) strongly suggest that this canal was used during a dry season (probably early summer). The relatively high abundance of *P. pustulosa* and *D. stevensoni* at high salinity intervals, like all samples in this canal, provides controversial evidence and unclear direction for their interpretation. However, both the paleoecologic salinity index and the trace metal salinity estimates are consistent, indicating one of the highest salinity records for all of the canals. This canal remained active throughout its entire record probably during the late spring to early summer. Little change in trace element data suggest that this canal reached stability soon after initial flooding. Toward the end of the canal history, temperature and salinity sharply increased to the highest values registered from any sample. (Keep in mind that the top of Feature 20 was truncated by modern activity and the higher levels of the canal were not its final use.) Water velocity estimates (1.5 m/s) proposed by Huckleberry (Chapter 20) are consistent with the high abundance of *I. bradyi* (stream ostracode), although his revised velocity of .9 m/s seems low for the occurrence of this species. However, no information on the species energy tolerance is known to allow further discussion on this matter. The presence of low percentages of cattail pollen in the canal's palynologic record is consistent with the suggested spring through early summer use.

Feature 21 was sampled from four strata deposited sometime after A.D. 990 or 1025, although a post A.D. 1200 date is also possible. This canal was subject to rapid salinization followed by gradual dilution.

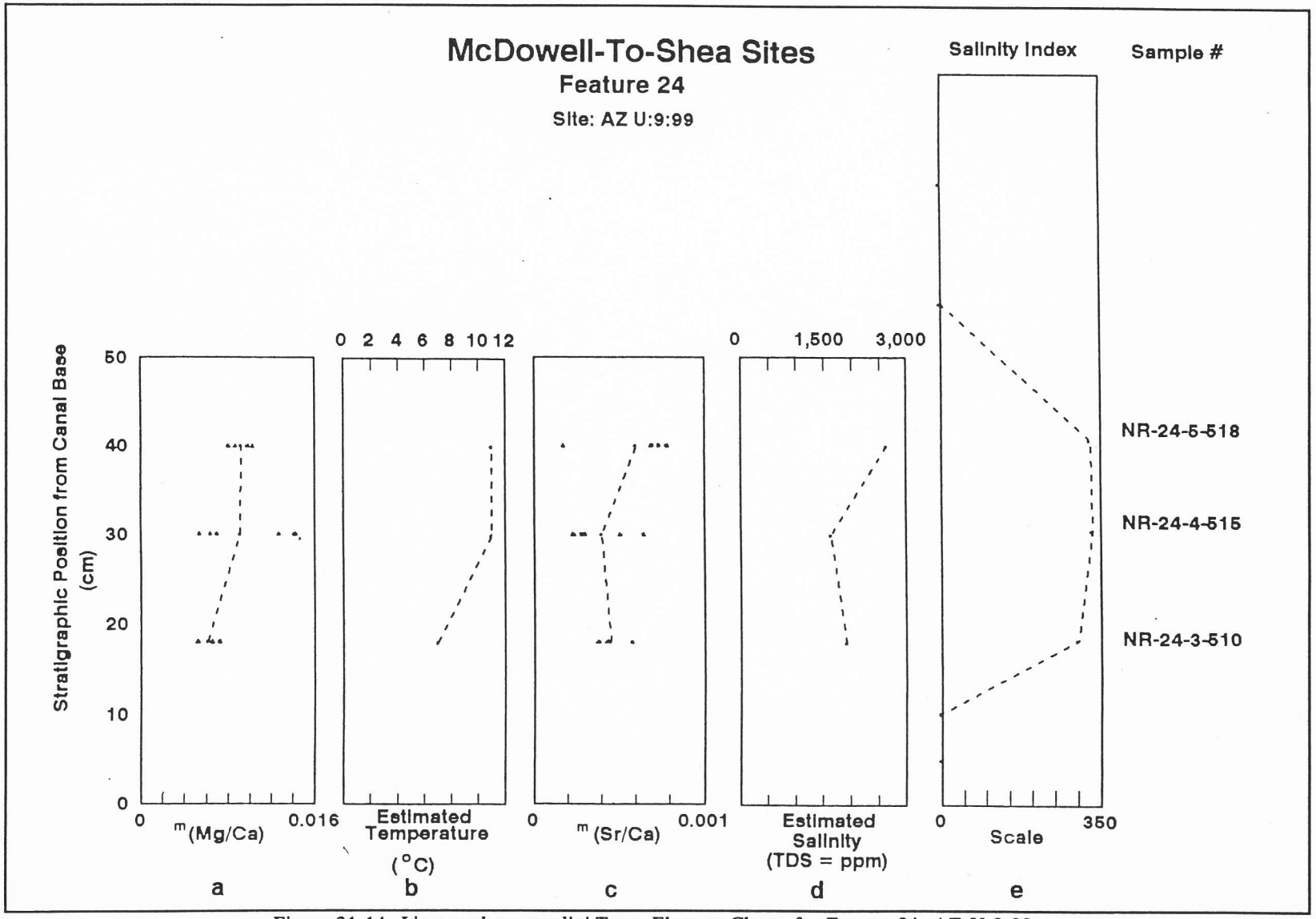

Figure 21.14 *Limnocythere staplini* Trace Element Charts for Feature 24, AZ U:9:99.

Table 21.12. Summary of Hohokam Canal Use during Pre-Classic and Classic Periods.

Feature	Age (A.D.)	Period	Canal Use	Season
22	700–990/1025	Colonial	Flooded with hypersaline waters (3,343–4,100 ppm) during the late spring (14–15°C). Canal water remained saline (4,529 ppm) probably because of stagnation or drought (14°C). Dilution occurred (2,719–1,870 ppm) during cooler conditions (8–10°C) probably of early monsoon. A new episode of salinization (2,489 ppm) resulted from stagnation during this time (9°C).	Late spring to early summer (pre-monsoon)
21	950–1050	Sedentary	Flooded with slightly saline waters (1,630 ppm) during the early spring (6–8°C). Rapid salinization (2,537 ppm) occurred probably because of stagnation and drought (?). Canal water dilution (1,148–1,765 ppm) resulted from headgate operation or winter-spring rainfall.	Late winter to early spring
24	1050–1200	Sedentary/ Early Classic	Flooded with high energy waters (ostracodes did not occur until canal stabilization). Stagnation or slow flow allowed a saline fauna. Salinity remained moderate (1,635–2,648 ppm) as temperature increased (7–11°C). A new high energy event destroyed fossil evidence and marks the end of the record.	Late winter to early spring
20	1200–1325	Early Classic	Flooded with saline waters (2,720–2,858 ppm) probably during the late spring (7–9°C). Warm and dry conditions prevailed and increased throughout canal use (salinity 3,084–5,038 ppm; temperature: 7–13°C).	Late spring to early summer (?)
23	1250–1325	Classic	Flooded with highly saline waters (3,331–3,500 ppm) during the late spring (11°C). The canal remained highly saline throughout its record (2,997–3,216 ppm) suggesting stagnation or saline water input. Apparent cooling (7–10°C) may resulted from pre- or early monsoonal rainfall. However, as a lateral canal, salinity and temperature values may demonstrate that canal waters become more saline as they flow away from source even during the spring.	Late spring to early summer (pre-monsoon) or spring
5	1250–1300	Classic	Flooded with saline waters (2,766 ppm) during the late winter/early spring (7–8°C). Further water input, either by headgate operation or winter-spring rainfall, diluted the canal waters (1,563–1,962 ppm) during the early spring (7–8°C).	Late winter to early spring
1	after 1290	Late Classic	Flooded with moderately saline waters (1,771–2,063 ppm) during the early spring (6–8°C). Slow flow or stagnant water during late spring (8–10°C) increased salinity (2,768–3,831 ppm). "Refreshening" event (salinity: 1,819–2,185 ppm; temperature: 6–7°C) probably resulted from headgate operation during the late spring.	Early to Late spring

During initial canal flooding, assemblage III was accompanied by slightly saline water. Although intermediate sample NR-21-3-434 is dominated by assemblage I, salinity did not vary significantly. The trace element record, however, shows a rapid increase in salinity (2,537 ppm) after initial runoff (NR-21-2-432). "Dilute" conditions (1,148–1,765 ppm) returned for the rest of the canal record. The combined record suggests that this canal was probably used sometime during the late winter to early spring. Temperature estimates of 5°–8° C and the paleosalinity index are almost constant throughout the canal history. The apparent increase in salinity shown by the ^{m}(Sr/Ca) ratio probably suggests a short cold-dry event. Canal activity was uninterrupted. Assemblage composition and geochemical data are in good agreement with Huckleberry's (Chapter 20) revised velocity estimates (.9 m/s). In contrast with Feature 20, Feature 21 contains a few specimens of *I. bradyi* suggesting low flow, thus the revised velocity is considered a likely possibility for this canal. The pollen

records include spring herbs and cattail, indicating spring to late spring canal use (Smith, Chapter 22).

The seven sampled strata of Feature 22 were within a pre-Classic period canal possibly used between A.D. 700 and 990/1025. Two episodes of water salinization and freshening are suggested. At the beginning of the canal operation, a rapid "freshening" episode is marked by the replacement of the initial assemblage I by assemblage IV. Similarly, the trace element data indicates that during this interval (NR-22-2-471) canal water salinity decreased (from 4,100 to 3,343 ppm). Then, salinization increased as shown by both the paleosalinity index and the ^{m}(Sr/Ca) ratio, probably to the highest levels recorded in this canal (4,529 ppm). However, the concordance between the paleoecologic and shell chemistry curves ends in this interval. The ^{m}(Mg/Ca) ratio trends show a slight temperature increase consistent with the dominance of *L. staplini* (NR-22-5-483). In contrast, the ^{m}(Sr/Ca) ratio for the same sample presents an opposite trend with respect to the paleosalinity index. Given the broad salinity tolerance of *L. staplini*, it is possible that this canal was subject to dilution during warm-wet events. The generally high salinity and temperature values (these are the highest temperatures recorded among the MTS canals) suggest that this canal was used during the late spring to early summer (pre-monsoon?), most likely at the end of a warm-dry season and the beginning of the warm-wet season. Ostracode records show that the flow regime was variable: decreasing rapidly, but then increasing, and slowing gradually toward the end of the canal history. Huckleberry (Chapter 20) proposes a constant velocity of 1.0 to 1.1 m/s. The pollen records are variable but flotation samples contained some specimens of elderberry (*Sambucus mexicana*) and ragweed (Ambrosiae) which are consistent with pre-monsoon interpretation from ostracodes (Smith, Chapter 22; Miksicek, Chapter 23).

Feature 23 was in use before A.D. 1325. It is the only canal suggesting constantly high salinity despite a rapid "freshening" episode recorded by sample NR-23-3-455 (assemblage I). The small size of the feature was undoubtedly influential in this regard. After initial flooding the canal remained saline (assemblage II). Salinity dropped, as suggested by the ostracode diversity in sample NR-23-3-455, but regained its high concentration almost immediately to conclude its record as a hypersaline water canal. Temperature and salinity estimates are strongly consistent with the paleoecologic record. Temperature decreased from 11° to 7° C, while salinity fluctuated between 2,997 and 3,500 ppm throughout the canal history, probably the narrowest range from all canals. The paleoecologic trend may reflect water permanence and flow energy instead of salinity. This pattern suggests that Feature 23 was most likely used during the late spring-early summer. Huckleberry (Chapter 20) estimates the lowest flow regime in the project area for this canal (.7 m/s). His estimates are consistent with the dominant occurrence of assemblage 1 and near absence of *I. bradyi* (this species occurs only at intervals suggesting water input). The pollen record is insufficient to make conclusions for this canal.

Feature 24, with sediments deposited between A.D. 1030 and 1210, had the least number of ostracodes for study; four of seven samples contained no ostracodes. Relatively high energy water flow conditions probably prevented ostracodes from becoming established in this canal until after the water flow was moderated. Once a moderate water flow was established, a saline water fauna assemblage grew in this canal. The water remained saline even though a more diverse fauna developed toward the middle use of the canal; the final use of the feature was devoid of carapaces. Trace element data generated temperature and salinity estimates congruent with the paleoecologic record for this feature. Temperature estimates rose from 7° to 11° C and remained constant for the rest of the canal's history. The canal TDS was moderately high during this time as salinity increased from 1,635 to 2,648 ppm. The diversity of ostracodes in the feature may have resulted from water stability (probably stagnant) and not from dilute water input. At the end of the canal's use, the disappearance of ostracodes from the record suggests that high energy water flow conditions prevented these organisms from hatching and becoming established. The combined records of Feature 24 suggest that it was used sometime during the late winter-early spring. Huckleberry (Chapter 20) proposes an average water velocity of 1.0 m/s; however, coarse sediments and lack of fossils at the beginning and end of the canal record suggest higher energy events. The palynologic record is consistent with this interpretation (Smith, Chapter 22).

DISCUSSION

Two primary aspects of the data presented in this research are discussed in the following section. First, the applicability of the experimentally derived constants to convert ^{m}(Mg/Ca) and ^{m}(Sr/Ca) ratios into temperature and salinity estimates are examined (Palacios-Fest

1994b). Second, the association of paleoenvironmental estimates with seasonal agricultural activity is discussed along with its implications for understanding the human/environment relationship. The environmental significance of the geochemical conversions is discussed first.

This study provides the first opportunity to combine ostracode paleoecology studies with temperature and salinity estimates that are generated from experimentally derived constants. Previously, interpretations were limited to speculation about the "cold-hot," "wet-dry," and "dilute-saline" conditions suggested by the trace element patterns. There was no data to correlate those trends to the physical and chemical characteristics of the water body (Palacios-Fest 1989, 1994a). The introduction of ^{m}(Mg/Ca) ratios in this study enable the reconstruction of water temperature at the time of valve calcification. If ostracodes follow the manner of other crustaceans and molt by dawn, then temperature estimates calculated for this study suggest an early morning water temperature (Martha Palacios-Fest, personal communication 1994). In turn, canal water temperatures probably reflect surface air temperatures because of the shallow nature of the canals. A detailed study on the molting processes of ostracodes is crucial to determine the validity of this assumption and to test the accuracy and significance of the temperature estimates proposed in this study.

The ^{m}(Sr/Ca) ratios in the valves allowed the reconstruction of the total dissolved solids concentration in water at the time of shell formation. Salinity approximations presented in this chapter are consistent with Palacios-Fest's (1994b) first calculations from Hohokam canals for the Classic period. Furthermore, these values are in good agreement with historic salinity records of the Salt River (Code 1900; Hem 1985; Ackerly 1989a). Water diverted from the Salt River to the irrigation system contained moderate levels of dissolved solids, but with pronounced seasonal and annual variations in the river's salt content (Ackerly 1989a). Ackerly (1989a) suggests that salinity would increase downstream on the Salt River and, consequently, toward the terminal ends of the canals themselves.

Ostracode paleoecology and shell chemistry can provide basic information about the dynamics of Hohokam irrigation systems and seasonal canal use. For example, the occurrence of *L. staplini* in most canals shows that a broad range of salinity (from freshwater to hypersaline conditions: 500–75,000 ppm) in slow motion to stagnant water bodies may have been present. However, in the Hohokam canals this species is usually associated with a diversity of other ostracodes unable to bear extremely high salinity (over 6,000 ppm). Some species are restricted to freshwater conditions (< 600 ppm), like *P. pustulosa* (Table 21.2). Other species, like *I. bradyi*, only grow in streams, so its occurrence in prehistoric canals is interpreted as evidence for either high energy conditions or proximity to headgates. Thus, the paleoecologic record provides a good approach to examine the canals' flow regimes and dilution-evaporation events. Independent confirmation of these water flows is supplied by Huckleberry (Chapter 20), with retrodicted water velocity estimates being in good agreement with the ostracode data.

Shell chemistry is also critical toward establishing what seasons the canals were most likely used. Temperature variation suggests the timing of canal use. For example, those canals that show increasing temperature values near the top of the record are considered as used sometime between late winter and late spring, whereas those canals showing the reverse pattern are interpreted as being used during mid-to-late summer. There is no indication that any of the MTS canals were in use after the late summer. Shell chemistry data suggests that the canals were used before the monsoon season. This interpretation is in good agreement with Ackerly (1989a), who suggests that during historic time (1895–1908) the Tempe Canal received its largest discharge from late February to early April, whereas the lowest discharges occurred between June-July and September-October.

Comparison of the ostracode and pollen data that was used as seasonal indicators of canal use also provides some independent confirmation of the conclusions. Information from Features 20, 22, and 23 have the most in common, with all three features showing some degree of spring to summer use. Less agreement is visible from Features 5, 21, and 24 where the ostracode data suggests a late winter and early spring water flow, but the pollen data indicates a springtime flow and some possible summer influxes. The lack of concordance between these two assessments may simply be the terms used by the separate investigators (e.g., late winter versus early spring). The feature with the least agreement of seasonal usage is Feature 1. The pollen data from Feature 1 suggests year-round use, whereas the ostracode data has a more restricted period of early to late spring use. Explaining this difference remains impossible at the present time.

Some problems related to temperature approximations remain unresolved. Estimations derived from the MTS canals appear lower than expected, particularly

for the late spring-late summer estimates. Two situations could account for these low values. First, ostracodes may molt during the early hours when water temperature is at its lowest level. Low spring temperatures are less than 8° C, while low summer temperatures range from 10° to 20° C (USDA climatologic records from Phoenix stations). Second, trace element analyses generated low ^{m}(Mg/Ca) ratios. The low Mg^{2+} results from what were assumed to be summer contexts could indicate laboratory errors. Although possible, this explanation is unlikely because all samples were prepared in a similar manner following a well-established laboratory procedure. Early morning mineral uptake by ostracode valves could explain the low Mg^{2+} results. However, these results require further analysis to verify their validity.

In summary, ostracode assemblages indicate that the canals underwent episodic salinization and freshening episodes throughout their history. An observation not reported before is that ostracode assemblages consistently recorded gradual "freshening" in most canals which ended abruptly with the canal record. Shell chemistry constants used in this study have proven their potential to inform about human-environment relationships. This approach could become more powerful with our better understanding of ostracode shell chemistry and physiology.